HHS Public Access

Author manuscript

J Immunol. Author manuscript; available in PMC 2020 June 15.

Published in final edited form as:

J Immunol. 2019 June 15; 202(12): 3434–3446. doi:10.4049/jimmunol.1801684.

ISWI ATPase Smarca5 Regulates Differentiation of Thymocytes Undergoing β-selection.

Tomas Zikmund[1], **Juraj Kokavec**[1], **Tereza Turkova**[1], **Filipp Savvulidi**[2], **Helena Paszekova**[1], **Sona Vodenkova**[3], **Radislav Sedlacek**[4], **Arthur I. Skoultchi**[5], and **Tomas Stopka**[1]

[1]Biocev; 1st Faculty of Medicine; Charles University; Czech Republic

[2]Institute of Pathological Physiology; 1st Faculty of Medicine; Charles University; Czech Republic

[3]Institute of Experimental Medicine; AS CR, v.v.i. & 3th Faculty of Medicine; Charles University; Czech Republic

[4]Czech Centre for Phenogenomics; Institute of Molecular Genetics; AS CR, v.v.i.; Czech Republic

[5]Department of Cell Biology; Albert Einstein College of Medicine; Bronx; NY

Abstract

Development of lymphoid progenitors requires coordinated regulation of gene expression, DNA replication and gene rearrangement. Chromatin remodeling activities directed by SWI/SNF2 superfamily complexes play important roles in these processes. Here we utilized a conditional knockout mouse model to investigate the role of Smarca5, a member of the ISWI subfamily of such complexes, in early lymphocyte development. *Smarca5* deficiency results in a developmental block at the DN3 stage of αβ thymocytes and proB stage of early B cells at which the rearrangement of antigen receptor loci occurs. It also disturbs development of committed ($CD73^+$) γδ thymocytes. The αβ thymocyte block is accompanied by massive apoptotic depletion of β-selected double negative DN3 cells and premitotic arrest of CD4/CD8 double positive cells. Although *Smarca5*-deficient αβ T cell precursors that survived apoptosis were able to undergo successful Tcrβ rearrangement, they exhibited a highly abnormal mRNA profile including persistent expression of CD44 and CD25 markers characteristic of immature cells. We also observed that the p53 pathway became activated in these cells and that a deficiency of p53 partially rescued the defect in thymus cellularity (in contrast to early B cells) of Smarca5-deficient mice. However, activation of p53 was not primarily responsible for the thymocyte developmental defects observed in the *Smarca5* mutants. Our results indicate that Smarca5 plays a key role in the development of thymocytes undergoing β-selection, γδ thymocytes, and also B cell progenitors by regulating transcription of early differentiation programs.

INTRODUCTION:

Production of mature T and B cells is a multistep process of differentiation from a multipotent progenitor that requires coordinated regulation of gene expression, replication,

CORRESPONDENCE: Dr. Tomas Stopka, Biocev, 1st Faculty of Medicine of the Charles University, Prumyslova 595, Vestec, 25242, Czech Republic; tstopka@lf1.cuni.cz.

DNA rearrangement and repair. Progenitors of T cells migrate from the bone marrow into the thymus where they respond to a new environment by initiating a transcriptional program of T cell specification, while proliferating extensively (1). During this process, $CD4^{-}CD8^{-}$ double negative (DN) $CD44^{+}$ positive early T lineage precursors (ETP or immature DN1) permanently silence the group of progenitor-related regulatory genes leading to gradual upregulation of CD25 and downregulation of c-Kit surface markers and resulting in the commitment completion at the end of the DN2 stage ($CD44^{+}CD25^{+}$c-Kit^{int}) (2). Thymocytes at the subsequent DN3 stage ($CD44^{-}CD25^{+}$) cease from cycling, and importantly undergo a random rearrangement of gene segments at the *Tcrb* locus and commence the expression of components related to β-selection program. Upon successful rearrangement that yields functional pre-TCR complexes, thymocytes proliferate rapidly, become rescued from the p53-regulated cell cycle arrest and apoptosis (3), and then are allowed to progress into the DN4 stage ($CD44^{-}CD25^{-}$). This transient population hence upregulates expression of CD4 and CD8 to become double positive (DP) cells and initiates *Tcra* locus rearrangement. DP cells with productive TCRαβ are positively and negatively selected so that only those with "proven" TCR can undergo differentiation into CD4 or CD8 single positive (SP) cells (4).

Eukaryotic cells evolved numerous epigenetic regulatory mechanisms of gene expression, DNA replication and repair to accomplish the T cell development. During early T cell differentiation NURD and SWI/SNF chromatin-remodeling complexes were shown to play important roles in both activating as well as silencing the gene transcription (5, 6). The SWI/SNF-related matrix-associated actin-dependent regulator of chromatin subfamily A member 5 (Smarca5, Snf2h) represents a widely expressed and conserved chromatin remodeling factor required for early development in mouse and lower organisms (7). Smarca5 is an ATPase from the ISWI subfamily that functions as a molecular motor for nuclear complexes that assemble and slide basic chromatin subunits, nucleosomes. Smarca5-containing complexes have diverse nuclear functions - guiding transcription of ribosomal (in NoRC and B-WICH complexes) and some coding genes (within the ACF or RSF complexes), participating in regularly spacing of the nucleosomal array before and after DNA replication, facilitating the recruitment of DNA repair machinery (CHRAC and WICH complexes) and finally orchestrating higher-order chromatin structure formation of centromeres and chromosomes (RSF) (8). While several members of SWI/SNF and CHD family have had their roles established in T cell development through studies involving gene inactivation mouse models, such a role for the ISWI subfamily has not been determined yet.

Currently, there is only a limited knowledge of how Smarca5, which is highly expressed in lymphocytes (9), participates in lymphopoiesis. We previously showed that deletion of the *Smarca5* gene resulted not only in the depletion of myelo-erythroid precursors, but also affected the earliest development of lymphoid progenitors in the mouse fetal liver (10). Additionally, Smarca5 was implicated in the V(D)J cleavage of the polynucleosomal substrate in a cell-free system (11). Another report implicated that Smarca5 in the ACF complex represses the interleukin receptor-α gene (CD25) via chromatin organizer Satb1 (12). Lastly, Smarca5 regulates expression of key interleukins (Il-2, Il-3, Il-5) in murine EL4 T cell lymphoma (13). While the role of Smarca5 in lymphopoiesis was previously suggested, the knockout models of Smarca5-interacting partners revealed no alterations in

lymphoid development including the deletion of *Acf1/Baz1a* (ACF and CHRAC complexes) (14, 15) or *Tip5/Baz2a* (NoRC) (15) genes in mice. Interestingly, it has been shown *in vitro* that Smarca5 can also remodel nucleosomes alone without being part of the complexes (16). As several of Smarca5-interacting partners are dispensable, studying the requirement of a catalytic subunit of the ISWI complexes by targeting experimentally Smarca5 during lymphoid development, may represent a successful strategy to reveal its function in lymphopoiesis.

We herein focused on deciphering the role of Smarca5 in thymocyte development and studied the molecular consequences of conditional Smarca5 deficiency in mice. Our work suggests that Smarca5 controls early T cell development by guiding early differentiation-coupled transcriptional programs at the DN3 stage and its deficiency results in thymocyte proliferation and survival defects through activation of the DNA damage response.

MATERIALS AND METHODS:

Mice

Smarca5^{flox} conditional knockout mice contain loxP1 sites flanking the exon 5 of the *Smarca5* gene (17) deletion of which produced a frame shift mutation (*Smarca5*^{del}) that disrupts expression of the Smarca5 protein. The murine strain expressing a codon-improved (iCre) recombinase under hCD2 promoter (B6.Cg-Tg(CD2-cre)4Kio/J) was purchased from the Jackson Laboratory. OT-II strain (B6.Cg-Tg(TcraTcrb)425Cbn/J) was kindly provided by Dr. Tomáš Brdička (Institute of Molecular Genetics, Prague). *Rag1* knockout (B6.129S7-Rag1tm1Mom/J) strain was kindly provided by Dr. Tomáš Brabec (Institute of Molecular Genetics, Prague). *Trp53* knockout strain (B6.129S2-Trp53tm1Tyj/J) was kindly provided by Dr. Winfried Edelmann (Albert Einstein College of Medicine, NY).

Flow cytometry

A single cell suspension from thymi and spleens of 4–6 week-old mice was obtained using a Dounce homogenizer. Cells were first preincubated for 10 min on ice with Fc receptor-blocking anti-CD16/32 (clone 93) antibody in PBS-1% biotin-free BSA solution and then stained for 20 min with specific primary antibodies. Biotinylated primary antibodies were revealed with streptavidin conjugated fluorescent dyes (SAv-PE/Cy7, SAv-APC, SAv-APC/Cy7). Labeled cells were analyzed on BD FACSCantoII (BD Biosciences) or CytoFLEX (Beckman Coulter) flow cytometers and data analysis was performed using FlowJo software (FlowJo, LLC). Clones of monoclonal antibodies were: anti-CCR6 (29–2L17), anti-CD3ε (145–2C11), anti-CD4 (GK1.5), anti-CD5 (53–7.3), anti-CD8 (53–6.7), anti-CD11c (N418), CD24 (M1/69), anti-CD25 (PC61), anti-CD27 (LG.3A10), anti-CD28 (E18), anti-CD44 (IM7), anti-CD45.1 (A20), anti-CD45.2 (104), anti-CD71 (RI7217), anti-CD73 (TY/11.8), anti-CD117 (c-Kit, 2B8) anti-B220 (RA3–6B2), anti-CD11b (Mac1, M1/70), anti-γδT-cell (GL3), hamster IgG-PE/Cy7 (HTK888), anti-Ly6G/Ly6C (GR1, RB6–8C5), anti-Nk1.1 (PK136), anti-Tcrβ (H57–597), anti-Tcrβ(Vα2) (B20.1), Ter-119 (all from Biolegend). Splenocytes were analyzed as previously described (18).

Bone marrow transplantation

For bone marrow (BM) reconstitution experiments 10^7 BM cells from adult (8 weeks old) control C57Bl/6J Ly5.1 (CD45.1) mice and *S5*$^{fl/fl}$hCD2iCre Ly5.2 (CD45.2) donors were reciprocally transplanted into lethally irradiated (7.5Gy) adult (8 weeks) S5$^{fl/fl}$hCD2iCre Ly5.2 and C57Bl/6J Ly5.1 control recipients, respectively. After one month post-transplantation, thymi were tested for the presence of donor-derived cell using flow cytometric analysis. The antibody panel included CD45.1, CD45.2, CD44, CD25, CD4, lineage cocktail (CD8, B220, Mac-1, Gr-1, Nk1.1, CD11c, Ter119) and CD45.1, CD45.2, CD4, CD5, CD8, lineage cocktail (B220, Mac-1, Gr-1, Nk1.1, CD11c, Ter119) for thymus.

BrdU/EdU labeling

Smarca5 conditional knockout mice and their age and gender-matched respective controls were intraperitoneally (i.p.) injected with 1 mg of 5-bromo-2´-deoxyuridine (BrdU) in 100 μl PBS. After 3 hours the thymocytes were isolated and antibody-stained for flow cytometry analysis or cell sorting. BrdU antigen recovery and its detection by fluorescently labeled antibody were performed using the APC BrdU Flow kit (BD Biosciences).

OP9/N-DLL1 stromal cell cultures

FACS sorted DN3 thymocytes (small CD4$^-$CD8$^-$CD25$^+$) and LSK (Lin$^-$Sca1$^+$Kit$^+$) bone marrow cells were cocultured with OP9 stromal cells expressing the Delta-like ligand (OP9/N-DLL1) in the presence of 1 ng/mL mIl-7 (407-ML-005) and 5 ng/mL hrFLT3 ligand (308-FK-005; PeproTech) as previously described (19). In bone marrow cells co-cultures, the concentration of Il-7 was lowered to 0.1 ng/mL from day 12 to allow differentiation. For CFSE labeling 3×10^4 DN3 cells were stained with 2.5μM CSFE following the manufacturer's guidelines (CellTrace™ CSFE cell proliferation kit, Invitrogen) and plated onto OP9 stromal cultures. Their proliferation and survival were analyzed by flow cytometry at 2, 4, 6 and 8 days of co-cultures. OP9/N-DLL1 cells were kindly provided by Hiroshi Kawamoto (Kyoto University).

Histopathology and detection of apoptotic cells in thymic sections

Thymi and spleens were fixed in 4% buffered formaldehyde for 48h, transferred in 70% ethanol, and paraffin embedded. Sections were obtained at 3 μm thickness and stained in H&E and Giemsa. Cleaved Caspase-3 was detected by immunohistochemistry utilizing a 1:1000 dilution of antibody (Abcam, ab52293) and visualized on a Zeiss Axio Scan.Z1. Casp3 positive cells were quantified using the Zen Blue Edition software (Zeiss).

RNA-seq analysis

CD4$^+$ CD8$^+$ (B220$^-$ Gr-1$^-$ Nk1.1$^-$ CD11c$^-$ CD11b$^-$) thymocytes were sorted by FACS and the total RNA was isolated using TRIzol Reagent (Invitrogen). DP cells pooled from 25–37 *S5*$^{fl/fl}$hCD2iCre thymi (each pool of 3×10^6 DP cells), 6 *S5*$^{fl/fl}$hCD2iCre *Trp53*$^{-/-}$ thymi (~2.5×10^6 DP cells/pool), and single non-pooled control thymi provided sufficient amounts of RNA for RNA-seq analysis. Strand-specific cDNA libraries were prepared from a minimum of 1.7μg of each DNAse treated (AM1906; Ambion DNA-free Kit) RNA sample using the TruSeq Stranded mRNA LT kit (Illumina). The RNA libraries were sequenced on

an Illumina HiSeq 2500 instrument in Rapid Run mode with paired-end 100bp sequencing length. Reads were mapped and aligned to mouse reference genome assembly GRCm38.p6 and transcripts were annotated and counted with Ensembl Release 94 (October 2018) using a HISAT2 aligner (20). The two RNA-seq technical replicates for each sample were combined. Differential expression analysis of RNA-seq data was performed in R Studio (21) using package DEseq2, which uses a median of ratios normalization method that accounts for sequencing depth as well as RNA composition (22). Volcano plots were drawn using ggplot2 (23) package in R suite. Expression levels (*TPM*, Transcripts Per Kilobase Million) for Ensembl 94 genes were calculated in R using gene lengths retrieved by EDASeq package (24) and in-house scripts. The shrinkage of $\log_2$ fold change values ($\log_2$FC) was estimated using DESeq2 lfcShrink function using the adaptive t prior shrinkage estimator “apeglm” (25). The RNA sequencing data is publicly available at the ArrayExpress database under accession number #E-MTAB-7758 (https://www.ebi.ac.uk/arrayexpress/experiments/E-MTAB-7758/).

q-*PCR*

Quantitative measurements of *Tcrb* rearrangement were done on gDNA (DNAeasy, Qiagen, USA) isolated from the FACS-sorted DN subpopulations. Quantitative PCR was run on 7900HT using Power SYBR Green PCR master mix (#4367659, ABI) with following primers *Dβ1*_fwd: 5´- GTGGTTTCTTCCAGCCCTCAAG-3´;*Dβ1*_rev: 5´- GGCTTCCCATAGAATTGAATCACC −3´; *Dβ2*_fwd: 5´- CAGGCTCTGGGGTAGGCAC-3´; *Dβ2*_rev: 5´- CCTCTTCCAGTTGAATCATTGTGG-3´. Primers for the control region were: *Apob*_ex29_fwd: 5´- CTGCCGTGGCCAAAATAAT-3´; *Apob*_ex29_rev: 5´- AATCCTGCAGATTGGAGTGG-3´. C_t values of *Dβ1* and *Dβ2* regions were normalized to C_t from *Apob* control region.

Immunoblotting

Freshly-isolated thymocytes were collected by centrifugation and resuspended in PBS with inhibitors of phosphatases (PhosSTOP, Roche) and proteases (cOmplete ULTRA, Roche). The cell suspension was then diluted 1:1 by adding solution of 50mM Tris-Cl (pH=8) and 2% sodium dodecyl sulfate (SDS) and incubated for 30 min at 97°C. Protein concentration was determined by BCA method (#23228, Pierce). Proteins were then resolved on SDS gradient 4–15% polyacrylamide gels (Mini-Protean TGX Stain-free gels, Bio-Rad) and wet-blotted (1h at 100V) onto PVDF membranes (#162–0177, Bio-Rad). PVDF membranes were blocked for 1h in 5% non-fat milk in TBS/0,1%Tween-20 (TBST) and incubated overnight at 4°C in 3%BSA/TBST 0,1% sodium azide with following antibodies: Smarca5 (1:1000, Bethyl, #A301–017A-1), histone H3 (1:1000, Abcam, #ab791). Membranes were 3 × 5min washed in TBST buffer at RT and incubated with peroxidase-conjugated F(ab’)2 antibody fragment either donkey anti-rabbit or donkey anti-mouse (1:10 000, Jackson Immunoresearch) in 5% non-fat milk in TBST for 1h. Membranes were 3 × 5min washed in TBST and the protein signal was visualized by Pierce SuperSignal West Femto Maximum Sensitivity substrate (Thermo Scientific) and detected with the ChemiDoc Imaging System (Bio-Rad).

RESULTS:

Smarca5 deficiency disrupts thymocyte development.

To delineate specific roles of Smarca5 *in vivo* we previously created the *Smarca5*^{fl} allele containing two loxP1 sites surrounding exon5, the deletion of which results in removing the portion of evolutionarily conserved helicase domain and introducing a frame-shift mutation (10, 17) (Fig. 1A). In order to execute the T cell specific deletion of the *Smarca5* gene, we crossed *Smarca5*$^{fl/fl}$ mice with hCD2iCre transgenic mice, in which the hCD2 promoter and locus control region (LCR) drive expression of the codon-improved Cre recombinase (26). Use of the hCD2-iCre transgene to study thymocyte development was chosen as this model alone caused no defect in thymus development (27) as well as the cellularity and subset composition of the major lymphoid organs (including thymus, spleen, and lymph nodes) did not differ between hCD2-iCre expressing mice and wild-type (28). We initially evaluated the onset of the *Smarca5*^{fl} gene deletion by PCR. Genomic DNA was prepared from FACS-sorted CD4/CD8 double negative (DN) thymocyte subpopulations of *Smarca5*$^{+/fl}$hCD2iCre mice and three primer sets amplifying wild-type, *Smarca5*-floxed (*S5*^{fl}) and recombined-floxed (*S5*^{del}) allele were used. Consistently with previous reports which used the hCD2iCre transgene (26) we observed Cre-mediated recombination of loxP1 sites as early as the DN1 stage in which the recombined *S5*^{del} allele was detectable (Fig. 1B). However, the deletion of the S5^{fl} allele at DN1 was only partial while its complete deletion was observed at the DN3 stage. Western blot analysis of the whole thymic cellular extracts from *S5*$^{fl/fl}$hCD2iCre mice confirmed a high efficiency of recombination as we observed marked reduction of Smarca5 protein levels (Fig. 1C).

S5$^{fl/fl}$hCD2iCre pups were born healthy and at normal Mendelian ratios. Following the third month of age, the *Smarca5* mutants however displayed rectal prolapses suggesting the disturbance of immune functions. Gross dissection of the *Smarca5* mutant animals revealed severe thymic defects. Thymi from the mutant mice were dramatically reduced in size and weight (Fig. 1D), which was reflected by a 17-fold reduction in cellularity (Fig. 1E). Histological evaluation revealed alteration of thymic corticomedullary architecture (Fig. 1F) and a higher number of cleaved Caspase-3 positive apoptotic death events in the cortex (Fig. 1G). Quantification of multiple cortical sections from different animals showed there was a 3-fold increase of apoptotic cells in the cortex of *S5*$^{fl/fl}$hCD2iCre thymi. These observations indicated a developmental defect in thymocytes accompanied by increased cell death within the thymi of *S5*$^{fl/fl}$hCD2iCre animals.

To gain insight into the developmental defects of thymocytes, we utilized flow cytometry of thymic cell suspensions of 4–6 weeks old *S5*$^{fl/fl}$hCD2iCre mice. CD4/CD8 immunostaining revealed a marked reduction of double positive (DP) and CD4-SP cell populations with a corresponding relative increase in DN thymocytes in the mutant thymi (Fig. 2A). In absolute counts, the DP cells were depleted by 60-fold, CD4-SP 90-fold, and CD8-SP cells 12-fold, whereas the DN thymocyte population was similar to controls (Fig. 2B). As the *Smarca5* allele deletion is completed by the DN3 stage (Fig. 1B) we analyzed each subpopulation of DN thymocytes in order to more precisely determine a stage, in which the block of development occurs. CD44/CD25 antigen expression profiles of lineage negative DN

thymocytes revealed a relative increase in DN3 cells to the detriment of DN4 thymocytes (Fig. 2C). Translated into absolute counts it was an almost complete absence of DN4 thymocytes in mutants while DN3 population was present in comparable numbers to controls (Fig. 2D).

We also examined the impact of Smarca5 deficiency on γδ T cell development. Using flow cytometry we observed that Smarca5 deficient animals contain twice as many Tcrδ$^+$ thymocytes (CD4$^-$CD8$^-$Tcrδ$^+$) compared to controls (Fig. 2E,F). However, out of these Tcrδ$^+$ thymocytes only 18.4% (compared to 42% in controls) were able to adopt the γδ fate (Fig. 2E) as indicated by the CD73 surface marker that discriminates Tcrδ$^+$ thymocytes committed to the γδ lineage (29). Additionally, the expression of surface CD24 antigen, which is normally enriched on immature γδ thymocytes and downregulated upon maturation into effector cells (30), was reduced in Smarca5 mutants (Fig. 2E). In contrast to controls, the lower expression of CD24 surface antigen observed in the mutants compromised a clear separation of the CD73$^+$ population into immature and mature subsets. The mature γδ thymocytes (CD24^{low}CD73$^+$) were further distinguished along the expression of the mutually exclusive CD27 and CCR6 surface markers into INF-γ(CD27$^+$)-producing or Il-17a(CCR6$^+$)-producing γδ subsets (31, 32). The IFN-γ and Il-17a-producing γδ subsets display a subtle imbalance in favor of Il-17a-producing subset in the Smarca5 mutants (Fig. 2E). We conclude that the commitment to γδ lineage, CD24 expression by Tcrδ$^+$ thymocytes, and development of mature γδ subsets are impaired in the *S5$^{fl/fl}$*hCD2iCre mice. Taken together, while Smarca5 plays important roles in thymocyte development during the DN3 to DN4 transition of αβ subsets it also guides the development of the γδ compartment.

Developmental blockade in Smarca5-deficient thymocytes is cell-autonomous.

As hCD2-iCre transgene initiates deletion also in other murine hematopoietic cell subtypes (18), we tested whether the DN3 to DN4 transition defect is cell autonomous to thymocytes or a result of impaired thymic microenvironment in which they develop. Utilizing syngeneic transplantation, we assessed the ability of control bone marrow (marked by CD45.1 isoform) to repopulate thymocytes in lethally irradiated *S5$^{fl/fl}$*hCD2iCre mice (marked by CD45.2 isoform) and vice versa. At day 35 after transplantation, we observed that engrafted thymocytes from controls (CD45.1) developed normally to produce CD4/CD8 double and single positive cells in the thymic microenvironment of *S5$^{fl/fl}$*hCD2iCre (CD45.2) animals (Fig. 3A,B). In turn, the engrafted donor *S5$^{fl/fl}$*hCD2iCre bone marrow-derived thymocytes (CD45.2) recapitulated the developmental defect at DN3 to DN4 transition within the control acceptor animals (CD45.1). These results suggested that the DN3 to DN4 transition became defective independently of the thymic stromal components (of *S5$^{fl/fl}$*hCD2iCre mice) but rather intrinsically to the thymocytes lacking Smarca5. To further settle the point whether the developmental defect of thymocytes observed *in vivo* is cell autonomous we utilized *ex vivo* co-cultures with a bone-marrow-derived stromal OP9/N-DLL1 cell line (19). Sorted preselection early DN3e cells (small CD4$^-$CD8$^-$CD25$^+$ thymocytes) were added on the OP9/N-DLL1 cells to evaluate the formation of DN4 and DP thymocytes in a time course of 8 days (Fig. 3C). While control DN3e cells apparently proliferated and progressed into more mature developmental stages under *ex vivo* conditions, the majority of Smarca5-

depleted cells were held at the DN3 stage till day 8 and their absolute numbers remained similar to the starting co-cultures (Fig. 3C,D). Thus, the outcome of the *ex vivo* experiment was highly reminiscent of the phenotype of *S5*$^{fl/fl}$hCD2iCre mice. We utilized yet another approach to test whether the defect of DN3 to DN4 transition could have emerged from a secondary effect, mainly because the DN3e thymocytes in the OP9/N-DLL1 co-cultures were sorted from *S5*$^{fl/fl}$hCD2iCre mice with the potentially impaired thymic microenvironment. We isolated LSK (Lin^{-}Sca-1^{+}c-Kit^{+}) bone marrow hematopoietic progenitors from *S5*$^{fl/fl}$hCD2iCre or control mice and kept them differentiating *ex vivo* on the OP9/N-DLL1 cells. Again, both the control as well as *S5*$^{fl/fl}$hCD2iCre-derived hematopoietic progenitor cells developed normally into the DN2 stage (day 9), however from the 16th day of culture, the *S5*$^{fl/fl}$hCD2iCre thymocytes were progressively underrepresented and by day 22 the DN3 to DN4 transition defect was revealed (Fig 3E,F). Thus, the loss of Smarca5 in developing T cells caused a defect intrinsic to the thymocytes undergoing DN3 to DN4 transition as evidenced by the co-cultures utilizing the OP9 cells and was not a result of a secondary effect due to impaired thymic stromal components or thymic microenvironment.

Smarca5-deficient thymocytes undergo marked apoptosis and proliferation impairment.

We next investigated whether reduced cell numbers in *S5*$^{fl/fl}$hCD2iCre thymi and *ex vivo* OP9/N-DLL1 co-cultures (Figs. 1E, 3D) may be attributed to premature cell death and/or impaired proliferation. As determined by flow cytometry, the *ex vivo* cultivation of purified DN3e thymocytes eventually resulted in a gradual increase of Annexin V positivity up to 71% by day 8 that did not exceed 15% in controls (Fig 4A), indicating that loss of Smarca5 induced apoptosis in developing T cell precursors. Similarly, we examined the effect of Smarca5 loss on the proliferation, by labeling purified DN3e thymocytes with the intracellular fluorescent dye (CFSE) immediately before plating them on OP9/N-DLL1 cells. As seen in Fig. 4B, the analysis of the CFSE signal dilution indicated that the DN control thymocytes proliferated rapidly *ex vivo*. Conversely, those DN cells that did survive the *ex vivo* conditions exhibited a decreased division rate confirming impaired proliferation of *S5*$^{fl/fl}$hCD2iCre thymocytes. We then utilized the BrdU incorporation assay to analyze the ability of Smarca5-depleted cells to progress through various stages of the cell cycle. After a 3h pulse of BrdU *in vivo*, we observed that the percentage of proliferating BrdU^{+} DN3 cells (after exclusion of post-replicative BrdU^{+} events) was almost the same in mutants as in controls (14.8% vs 15.8%) and thus the G1-to-S progression was not altered after Smarca5 loss at DN3 stage (Fig. 4C). However, the portion of postreplicative cells at this stage, that is defined as strictly diploid BrdU^{+} events (33), was 2.5-fold decreased in mutant DN3 cells. These data indicate that Smarca5-depleted DN3 cells normally enter S phase and begin to replicate their DNA, however they are limited in completing the cell cycle to re-emerge as G1 cells. Mutant DP cells were also impaired as a substantial fraction of the DP cells became arrested at the G2/M phase (Fig. 4D). Thus, the developmental defects observed upon loss of Smarca5 are likely the consequence of cell death and impaired cell cycle progression at late S through G2/M phase. This is in contrast to defects in G1/S checkpoint mechanisms as previously observed in human cancer cell lines upon *SMARCA5* knockdown (34).

Smarca5 mutants undergo pre-TCR signaling and the TCR rearrangement.

The accumulation of Smarca5-depleted DN3 cells resembles the phenotype of mice that have a defect in pre-TCR signaling or *Tcrb* locus rearrangement (35). To test whether induction of pre-TCR signaling was affected by a loss of Smarca5, we performed intraperitoneal injections of anti-CD3ε antibody into $S5^{fl/fl}$hCD2iCre and into recombination-activating gene 1 ($Rag1^{-/-}$) deficient mice. Anti-CD3ε Ab can mimic pre-TCR signaling *in vivo* and stimulates preselection DN3 thymocytes to proliferate and differentiate into the DN4 cells even in the $Rag1^{-/-}$ mice lacking the Tcrβ chain expression (36). We observed, that the anti-CD3ε Ab stimulated downregulation of surface CD25 molecule on $Rag1^{-/-}$ as well as on Smarca5-deficient DN3 thymocytes (Fig. 5A), which suggested that pre-TCR signaling pathway was not disrupted after Smarca5 loss. However, we noted that compared to highly proliferating $Rag1^{-/-}$ DN cells the $S5^{fl/fl}$hCD2iCre DN cells were almost completely absent at day 2 of treatment (Fig. 5B), further confirming the poor survival of differentiating and proliferating Smarca5-deficient DN cells. We next examined the expression of CD2 and CD5 on the DN and DP cells to assess their upregulation upon pre-TCR signaling (37, 38). Data from flow cytometry show that β-selected DN cells that survived Smarca5 loss are still capable of upregulating the expression CD2 and CD5 molecules (Supplemental Fig. 1A). Additionally, at the DP stage, the expression of these molecules was almost identical as compared to controls (Supplemental Fig. 1B). In summary, the ability of $S5^{fl/fl}$hCD2iCre DN cells to upregulate CD2 and CD5 indicated that Smarca5 deficiency in thymocytes does not perturb the pre-TCR signaling.

Next, we analyzed the intracellular expression and rearrangement of the Tcrβ chain, another prerequisite for the DN3 to DN4 transition. Analysis of intracellular (i)Tcrβ expression together with membrane-bound CD28 has been shown as a tool to distinguish between preselection and β-selected DN3 cells that have successfully rearranged their *Tcrb* locus (39). Using this approach, we observed that mutant DN3 thymocytes contain a significantly reduced fraction of $iTcr\beta^{+}/CD28^{+}$ β-selected cells compared to controls (Fig. 5C). Conversely, the genomic DNA analysis of the *Smarca5* mutant DN thymocytes by quantitative PCR showed that the recombination rate of Dβ1-Jβ1 and Dβ2-Jβ2 gene segments was not altered (Supplemental Fig. 1C). As determined by RNA-seq analysis of DP cells (see further), also expression pattern of the constant (*Trbc)* and variable (*Trbv)* gene segments was similar to controls (Supplemental Fig. 1D) indicating that Smarca5 deficiency did not abolish the *Tcrb* locus rearrangement. To test whether the defective formation of the β-selected DN3 cells was a result of impaired Tcrβ rearrangement, we crossed $S5^{fl/fl}$hCD2iCre mice with *Tcrb/a* transgenic mice (OT-II). Expression of the fully rearranged *Tcrb/a* construct in OT-II background is able to suppress V(D)J recombination at endogenous loci and also “rescue” thymocyte development in mice lacking essential factors for the Tcrβ/α rearrangement (40, 41). Analysis of $S5^{fl/fl}$hCD2iCre OT-II animals revealed that expression of the transgenic Tcrβ/α chains failed to rescue the *Smarca5* knockout phenotype. The absolute and relative counts of DN and DP subpopulations remained similar to the $S5^{fl/fl}$hCD2iCre mice (Fig. 5D,E,F). Particular exceptions were mature SP thymocytes, where the CD4 SP cells whose 3-fold increase to the detriment of the CD8 SP cells likely reflected the positive selection of thymocytes towards CD4 lineage that normally occurs in the OT-II strain (Fig. 5D). Thus, rather the poor survival of β-selected DN cells

than defects in pre-TCR signaling or *Tcrb* locus rearrangement could best explain the phenotype of $S5^{fl/fl}$hCD2iCre mice.

As the surface expression of Tcrβ in DP thymocytes is essential for production of SP subpopulations, we focused on stages beyond DN3 to decipher how Smarca5 deficiency influenced the *Tcrb* expression. Normally, the surface expression of Tcrβ is low or none in the DN3 stage, becomes induced at the DN4 stage, and further upregulated in SP thymocytes. We examined the level of surface Tcrβ expression on individual developmental stages of thymocytes and mature peripheral T cells in the spleen. We observed that surface Tcrβ expression was detectable in all developmental stages from a subfraction of DN3 (low expression) to mature SP populations (high expression) in both Smarca5-deficient as well as control thymocytes (Fig. 5G, Supplemental Fig. 1E). However, the fraction of cells with upregulated Tcrβ expression was reduced within each analyzed Smarca5-deficient thymic subpopulation compared to controls. Taken together, Smarca5 deficient thymocytes are able to express and upregulate the surface Tcrβ expression during their development with exception at DN4 stage that almost lacks fraction of Tcrβ positive cells.

Smarca5 deficiency altered the developmental program of post-β-selection stages.

It has been shown that during differentiation from DN to DP stage, the ACF complex containing Smarca5 and Acf1 represses in cooperation with Satb1 the *Il2ra* (CD25) gene (12, 42). Indeed, flow cytometry indicated that DP cells of $S5^{fl/fl}$hCD2iCre mice inappropriately express both CD44 and CD25, the markers of earlier developmental stages. While the CD25 molecule becomes partially downregulated, the CD44 remains upregulated in DP cells implicating the dysregulation of early expression programs (Fig. 6A). Our previous studies suggested that Smarca5 participates in the regulation of gene expression programs associated with survival and differentiation of lens, cerebellum and hematopoietic progenitor cells (10, 17, 43). To gain a global view on the gene expression programs dysregulated by Smarca5 loss in β-selected thymocytes, we purified DP cells from $S5^{fl/fl}$hCD2iCre mice and used RNA-seq to compare the gene expression profiles with those from control DP cells. Of > 21.500 expressed genes, a total of 3.318 transcripts were differentially expressed with false discovery rate FDR<0.05 and BaseMean value >10. From these, 1.503 mRNAs were (<2 fold) downregulated and 1.815 mRNAs were (>2 fold) upregulated. Gene ontology analysis of the differential expression using *Gene Set Enrichment Analysis* (*GSEA*) (44) showed enrichment of mRNAs involved in expected categories such as apoptosis and the p53 pathway however most of them were either immunologic or lymphocyte-associated (Fig. 6B). By dividing the differentially expressed genes into previously published mRNA clusters with similar behaviors during thymocyte differentiation (45) we observed that the group of upregulated genes in the mutant DP cells overlapped to those mRNAs that peaked in expression at the early (DN1-DN2) or pre-β-selection DN3a stage (Fig. 6C). Such genes were for example receptors (*Il7r, Ctla4*, *Ptcra*, *Ly6a* and also *Il2ra*/Cd25 and *Cd44*), signaling molecules: (*Dtx1, Hes1, Notch1, Lfng, Rab44*) and transcription factors (*Irf7, Tcf7l2, Spib*) (Fig. 6D). Accordingly, the group of downregulated genes (total 97) fall into the category of genes which are gradually expressed by β-selected cells during transition into DP such as transcription factors (*Klf7, Ets2, Ikzf3, Bcl6*), surface molecules (*Plxnd1, Slamf1, Cd81*), signaling (*Themis*) and others (*Tdrd5,*

Cacna1e). To evaluate whether the mutant DP cells more closely resembled pre- or post-β-selected cells, we used a previously published transcriptome analysis of microarray data of wild-type C57Bl/6J DN3a and DP stage cells (45) and created two sets of 200 most upregulated and downregulated genes in wild-type (wt) DN3a compared to wt DP stage (Supplemental Fig. 2A). Hence the GSEA analysis of mRNAs dysregulated upon Smarca5 deficiency revealed a strong enrichment of upregulated (NES=2.37, FDR<0.001) and downregulated (NES=−2.53, FDR<0.001) mRNAs of the wt DN3a stage (Fig. 6E). This finding indicates that although Smarca5-deficient cells express post-β-selection surface markers (e.g. CD4, CD8, CD5, CD2) as normal DP cells, RNA-seq data reveals that they retain a transcriptional program of pre-β-selection DN cells. Thus, *Smarca5* ablation greatly disorders developmental programming of T cell progenitors.

Smarca5 is required for proB/preB transition of B cell progenitors.

Additional analysis of $S5^{fl/fl}$hCD2iCre mice revealed also a dramatic reduction of the spleen cellularity (Fig. 7A). Besides the reduction of splenic T cells and NKT cells, which both developed in the thymus from the $CD4^+CD8^+$ DP precursors (46), we also observed a marked depletion of B lymphocytes, while the numbers of myeloid cells were not significantly altered (Fig. 7B,C). Indeed, immunohistochemistry of mutant spleens showed prominent follicular hypoplasia affecting both T cell as well as B cell zones (Fig. 7D) suggesting also a defect in the B cell development of $S5^{fl/fl}$hCD2iCre mice. To investigate a stage at which the developmental defect occurred, the early B cell progenitor populations from bone marrow (BM) were analyzed. Flow cytometry analysis revealed almost complete loss of pre-B cells ($B220^+CD43^-$) in mutants, while the proportion of pro-B cells ($B220^+CD43^+$) was virtually unperturbed (Fig. 7E). Closer examination of the pro-B population showed a developmental arrest between early preselected pre-B-I cells ($CD117^+$) and pre-B-II ($CD25^+$) cells that underwent productive IgH gene loci rearrangement (47). Taken together, Smarca5 deficiency affects development of early $B220^+CD43^+$ pro-B cells in BM implicating the requirement of Smarca5 for both early T as well as B lymphocyte development.

p53 guides survival in the Smarca5-depleted thymocytes undergoing β-selection.

It has been previously noted that deletion of *Smarca5* gene in hematopoietic progenitors induces expression of p53 transcriptional targets (10). Our current RNA-seq data suggested that increased cell death and impaired cell cycle progression of thymocytes coincide with the activation of the p53 program (Fig. 8A). To test the biological significance and requirement of the *Trp53* gene for the *Smarca5* mutant phenotype in developing lymphocytes, we utilized an additional mouse strain homozygous for the *Trp53* null allele (48) to create the $S5^{fl/fl}$hCD2iCre $Trp53^{-/-}$ mice. Interestingly, the *Smarca5* deletion slightly prolonged the survival of the *Trp53* knockout mice (Fig. 8B). We observed that the introduction of the *Trp53* knockout allele improved thymic cellularity of the Smarca5-deficient mice (Fig. 8C). Flow cytometry analysis revealed a proportional increase (from 26.3% to 55.1%) as well as absolute cell number expansion (4-fold) of the double knockout DP population (Fig. 8D,E), while the absolute numbers of DN cells were unchanged indicating a DN to DP transition rescue (Fig. 8E,F). We performed RNA-seq of samples derived from the double knockout DP cells and compared gene expression profiles with previous data. Expression analysis

confirmed that the p53 targets especially those that are associated with induction of apoptosis in response to DNA damage such as *p21/Cdkn1a*, *Noxa/Pmaip1*, *Bax* were upregulated specifically in the Smarca5-deficient DP cells while upon the introduction of the *Trp53*$^{-/-}$ allele their expression became normalized (Fig. 8G). Although the thymic cellularity in double knockouts was partially recovered, we still observed markedly dysregulated expression of the mRNAs connected to normal thymocyte development (Supplemental Fig. 2B). Thus, the activation of p53 targets was rather a modifier of the severity of the phenotype and not contributory to differentiation defects observed in *S5*$^{fl/fl}$hCD2iCre mice. Indeed, flow cytometry analysis showed that *Smarca5* and *Trp53* double knockout DP cells contained up to a 3.5-fold excess of H3S10^{phos} positive (mitotic) cells as compared to single *Smarca5* knockout (Fig. 8H). However, the G2/M blockade in the DPs of the *Smarca5* and *Trp53* double knockout mice persisted (Supplemental Fig. 2C).

To test whether the p53 loss could also recover the development of early B cell progenitors, BM cells from *S5*$^{fl/fl}$ hCD2iCre mice with or without *Trp53*$^{-/-}$ loci were analyzed for the expression of B220 and CD43 molecules. However, unlike the partial rescue observed in the thymocyte compartment, the data from flow cytometry show that the p53 loss failed to rescue the survival and/or maturation at pro-B (B220^{+}CD43^{+}) to pre-B stage (B220^{+}CD43^{-}) transition (Fig. 8I). To conclude this part, the introduction of the *Trp53* knockout allele into the Smarca5-deficient strain significantly improved the proliferation and/or survival of thymocytes but not of early B cells. Importantly, the rescue experiment was unable to restore the dysregulated differentiation pathways in both B and T lineages.

DISCUSSION:

Although the SWI/SNF and CHD chromatin remodeling factors have been implicated in the regulation of lymphocyte progenitor-specific transcription and differentiation (6, 49), the role of ISWI proteins in the development of early T and B cells has not been addressed. This study brings yet unknown evidence that the ISWI ATPase Smarca5 regulates early lymphocyte development by promoting stage-specific gene expression, and secondarily, cell survival and proliferation. Interestingly, the role of Smarca5-containing remodeling complexes was previously implicated in the DNA double-strand break (DSB) repair in human immortalized cell lines (50, 51). These reports showed that SMARCA5 is rapidly recruited to DSBs and the knockdown of SMARCA5 sensitizes cells to DNA damage. SMARCA5 protein was shown recruited to the sites of DSB by histone deacetylase Sirtuin 6 (SIRT6) (51). Additional pathways and interaction partners of Smarca5 participating at the sites of DNA damage were also established (52, 53). Thus, Smarca5 seemed to be a suitable candidate for testing its *in vivo* role in lymphocytes, in which the developmentally programmed DSBs occur. Indeed, our data showed that *S5*$^{fl/fl}$hCD2iCre mice initially exhibited a marked reduction of those early progenitors that productively rearranged antigen receptor loci – the Tcrβ expressing DN3 thymocytes (Fig. 5C) and B220^{+}CD43^{+}CD25^{+} early B cells (Fig. 7E). Coincidently the upregulation of p53 target genes (Fig. 8G) and the partial recovery of thymus cellularity in the *S5*$^{fl/fl}$hCD2iCre *Trp53*$^{-/-}$ mice (Fig. 8C) could also be interpreted as Smarca5 being involved in the DSB repair during the antigen-receptor gene rearrangement. However, further experiments challenged this view. The developmental defect, at least in thymocytes, could not be attributed mainly to the DSBs repair aberration,

as the OT-II transgene was unable to rescue the DN3 to DN4 transition defect of Smarca5-deficient cells (Fig. 5D). Notably, the data from RNA-seq showed that the expression pattern of the constant (*Trbc)* and variable (*Trbv)* gene segments was similar compared to the control DP cells (Supplemental Fig. 1D) indicating that the relative utilization of the different gene segments during Tcrβ rearrangement was not affected in the mutants. In addition, the $S5^{fl/fl}$hCD2iCre $Trp53^{-/-}$ mice displayed comparable life span as $S5^{fl/fl}$ $Trp53^{-/-}$ mice (Fig. 8B), which is contrasting to the mouse knockout models of genes employed directly in the NHEJ that upon co-deleting with the *Trp53* accelerated tumorigenesis with shortened animal survival (54). Thus, the *Smarca5* deletion-mediated maturation defect is not primarily mediated via the disrupted repair of developmentally programmed DSBs.

Generally, except in the SP CD8 and CD4 T cells that expressed lower level of surface Tcrβ (Fig. 5G, Supplemental Fig. 1E), the iTcrβ expression and proximal pre-TCR signaling seem to be preserved in the Smarca5-deficient mice, as $S5^{fl/fl}$hCD2iCre DN3 cells gave rise (albeit with very low rate) to some DP-like cells and could be normally stimulated by anti-CD3 antibody. The DN3 stage and all the following developmental stages were considerably altered in the $S5^{fl/fl}$hCD2iCre mice. Once *Smarca5* was inactivated, β-selected DN3, DN4, DP and also pre-B cells lost their ability to accumulate and became depleted. Smarca5 loss leads to a marked increase in the number of cells undergoing apoptosis (Fig. 1G). Our data indicate that this was not caused by the induction of a generalized apoptotic response, as resting DN3e cells displayed very low level (up to 5%) of cell deaths even after 6 days of *ex vivo* cultivation (data not shown). This result together with the observation that Smarca5-deficient DN3 stage lacks postreplicative cells (Fig. 4C) rather suggested that the disruption of Smarca5 function triggers apoptosis of highly proliferating cells and especially those that have already entered the S phase. Others reported that depletion of Smarca5 in murine lens (using Le-Cre system) results in a reduction of BrdU and Ki67 positive presumptive lens epithelial cells leading to the lens developmental defect (43). Also, the early deletion of Smarca5 in cerebellar progenitors (using the Nestin-Cre system) resulted in a lower number of BrdU positive Purkinje cells and of granule neuron progenitors at E17.5 possibly due to massive cell death (17). Moreover, the defective S phase progression in the DN3 stage could also explain the formation of G2/M arrested $S5^{fl/fl}$ hCD2iCre DP cells (Fig. 4D). In the erythroid cell compartment, the Smarca5 loss caused the emergence of tetraploid cells permanently exiting cell cycle in populations of highly proliferating proerythroblasts-to-basophilic erythroblasts (10). This, along with a substantial number of apoptotic events was interpreted mainly as a consequence of activation of DNA damage-associated p53 program. Indeed, stressed replicating cells activate their replication checkpoint to delay S phase progression and G2/M transition (55). The p53 and its downstream molecules are then required to maintain a G2 or tetraploid G1 arrest which afterward promotes cell senescence (56–58). However, although $S5^{fl/fl}$hCD2iCre DP cells also upregulated some proapoptotic (*Noxa, Bax, Puma*) and cell cycle regulating (*Cdkn1a/p21*) p53 target genes, the rescue of phenotype was incomplete and the tetraploid events were still present in the *Smarca5* and *Trp53* double knockouts (Supplemental Fig. 2C) indicating that the cell cycle arrest and induction of apoptosis were predominantly p53-independent.

We hypothesize that the dysregulated expression of the stage-specific mRNAs (including the surface markers) in Smarca5-depleted β-selected cells stay behind the thymocyte defects observed in the *S5*$^{fl/fl}$hCD2iCre mice. Indeed, the ablation of chromatin remodelers Brg1 or Chd4/Mi-2β leads to differentiation defects, cell cycle arrest or apoptosis in β-selected thymocytes partially due to dysregulated gene expression (reviewed in 59). Unlike the Brg1 or Chd4 chromatin remodelers that regulate differentiation from DN4 to DP stages (60, 61), the *Smarca5* knockout phenotype appears early and relatively unique as the pre-β-selected DN3 cells lacking Smarca5 are unable to downregulate marker molecules (CD25, CD44). Among mechanisms behind inappropriate CD25 molecule expression might be the previously reported participation of Smarca5 in the Satb1 directed repression of *Il2ra/Cd25* loci (12, 42). Genome-wide characterizations of binding into chromatin by ChIP-seq revealed that Smarca5 is enriched mostly at the gene promoters and the regulatory regions (62, 63). Transcriptome analysis by RNA-seq confirmed a considerable number of ectopically expressed transcripts associated with β-selection and also genes that were not activated and remained downregulated during the transition into the DP stage (Fig. 6D) suggesting that the absence of Smarca5 disables a crucial component of the β-selection transcription machinery. The function of Smarca5 as a transcriptional activator and repressor was shown in studies using murine EL4 T-lymphoma cell line upon siRNA-mediated depletion. Although Smarca5 participates in repression of interleukin genes including *Il2*, *Il5*, *Il13*, *Il17a* and in activation of *Il3* after stimulation with PMA and ionomycin (13), we have not observed this during the transition into the DP stage as those interleukins are expressed mainly by mature T cells. Perturbation of Smarca5 functions may have also affected other profiles during the transition from pre- to post-β-selected DN3 thymocytes by dysregulating genes related to proliferation, metabolism, and β-selection (45). To conclude, Smarca5 represents an important transcriptional regulator that participates indispensably during early T cell development. To further address the role of Smarca5 in regulating T cell promoters we are currently preparing a transgenic mouse line with tagged Smarca5 protein.

Supplementary Material

Refer to Web version on PubMed Central for supplementary material.

ACKNOWLEDGEMENTS:

We thank Christian Lanctôt and Vladimír Divoký for helpful discussion, Ivan Kanchev for histopathology reports, Emanuel Nečas and Martin Molík for CD45.1 mice and assistance with the bone marrow transplantations, Dana Mikulenková and Ilona Jirasková for cytospin preparations, Luděk Šefc for help with flow cytometry analysis, Jan Kubovciak for help with RNA-seq analysis, and Martin Drobiš for style & writing.

GRANT SUPPORT:

StopkaLab & Biocev support: GAUK 534212, GACR 18–01687S and 19–03586S, AZV 16–27790A, UNCE/MED/016, KONTAKT LH15170, LM2015040 & NPU II LQ1604 (MEYS) and OP RDI CZ.1.05/2.1.00/19.0395 & CZ.1.05/1.1.00/02.0109 (ERDF, MEYS), PROGRES Q26, SVV 260374/2017. SV support: GACR 19–10543S and AZV 17–30920A. AIS support: NIH GM116143 and DK096266.

REFERENCES:

References

Uncategorized References

1. Rothenberg EV, Moore JE, and Yui MA. 2008 Launching the T-cell-lineage developmental programme. Nat Rev Immunol 8: 9–21. [PubMed: 18097446]
2. Zhang JA, Mortazavi A, Williams BA, Wold BJ, and Rothenberg EV. 2012 Dynamic transformations of genome-wide epigenetic marking and transcriptional control establish T cell identity. Cell 149: 467–482. [PubMed: 22500808]
3. Haks MC, Krimpenfort P, van den Brakel JH, and Kruisbeek AM. 1999 Pre-TCR signaling and inactivation of p53 induces crucial cell survival pathways in pre-T cells. Immunity 11: 91–101. [PubMed: 10435582]
4. Shah DK, and Zuniga-Pflucker JC. 2014 An overview of the intrathymic intricacies of T cell development. J Immunol 192: 4017–4023. [PubMed: 24748636]
5. Winandy S 2005 Regulation of chromatin structure during thymic T cell development. J Cell Biochem 95: 466–477. [PubMed: 15832342]
6. Dege C, and Hagman J. 2014 Mi-2/NuRD chromatin remodeling complexes regulate B and T-lymphocyte development and function. Immunol Rev 261: 126–140. [PubMed: 25123281]
7. Tsukiyama T, Palmer J, Landel CC, Shiloach J, and Wu C. 1999 Characterization of the imitation switch subfamily of ATP-dependent chromatin-remodeling factors in Saccharomyces cerevisiae. Genes Dev 13: 686–697. [PubMed: 10090725]
8. Erdel F, and Rippe K. 2011 Chromatin remodelling in mammalian cells by ISWI-type complexes--where, when and why? FEBS J 278: 3608–3618. [PubMed: 21810179]
9. Wurster AL, and Pazin MJ. 2008 BRG1-mediated chromatin remodeling regulates differentiation and gene expression of T helper cells. Mol Cell Biol 28: 7274–7285. [PubMed: 18852284]
10. Kokavec J, Zikmund T, Savvulidi F, Kulvait V, Edelmann W, Skoultchi AI, and Stopka T. 2017 The ISWI ATPase Smarca5 (Snf2h) is required for proliferation and differentiation of hematopoietic stem and progenitor cells. Stem Cells.
11. Patenge N, Elkin SK, and Oettinger MA. 2004 ATP-dependent remodeling by SWI/SNF and ISWI proteins stimulates V(D)J cleavage of 5 S arrays. J Biol Chem 279: 35360–35367. [PubMed: 15201272]
12. Yasui D, Miyano M, Cai S, Varga-Weisz P, and Kohwi-Shigematsu T. 2002 SATB1 targets chromatin remodelling to regulate genes over long distances. Nature 419: 641–645. [PubMed: 12374985]
13. Precht P, Wurster AL, and Pazin MJ. 2010 The SNF2H chromatin remodeling enzyme has opposing effects on cytokine gene expression. Mol Immunol 47: 2038–2046. [PubMed: 20471682]
14. Dowdle JA, Mehta M, Kass EM, Vuong BQ, Inagaki A, Egli D, Jasin M, and Keeney S. 2013 Mouse BAZ1A (ACF1) is dispensable for double-strand break repair but is essential for averting improper gene expression during spermatogenesis. PLoS Genet 9: e1003945. [PubMed: 24244200]
15. Koscielny G, Yaikhom G, Iyer V, Meehan TF, Morgan H, Atienza-Herrero J, Blake A, Chen CK, Easty R, Di Fenza A, Fiegel T, Grifiths M, Horne A, Karp NA, Kurbatova N, Mason JC, Matthews P, Oakley DJ, Qazi A, Regnart J, Retha A, Santos LA, Sneddon DJ, Warren J, Westerberg H, Wilson RJ, Melvin DG, Smedley D, Brown SD, Flicek P, Skarnes WC, Mallon AM, and Parkinson H. 2014 The International Mouse Phenotyping Consortium Web Portal, a unified point of access for knockout mice and related phenotyping data. Nucleic Acids Res 42: D802–809. [PubMed: 24194600]
16. He X, Fan HY, Garlick JD, and Kingston RE. 2008 Diverse regulation of SNF2h chromatin remodeling by noncatalytic subunits. Biochemistry 47: 7025–7033. [PubMed: 18553938]
17. Alvarez-Saavedra M, De Repentigny Y, Lagali PS, Raghu Ram EV, Yan K, Hashem E, Ivanochko D, Huh MS, Yang D, Mears AJ, Todd MA, Corcoran CP, Bassett EA, Tokarew NJ, Kokavec J, Majumder R, Ioshikhes I, Wallace VA, Kothary R, Meshorer E, Stopka T, Skoultchi AI, and

Picketts DJ. 2014 Snf2h-mediated chromatin organization and histone H1 dynamics govern cerebellar morphogenesis and neural maturation. Nat Commun 5: 4181. [PubMed: 24946904]

18. Siegemund S, Shepherd J, Xiao C, and Sauer K. 2015 hCD2-iCre and Vav-iCre mediated gene recombination patterns in murine hematopoietic cells. PLoS One 10: e0124661. [PubMed: 25884630]
19. Holmes R, and Zuniga-Pflucker JC. 2009 The OP9-DL1 system: generation of T-lymphocytes from embryonic or hematopoietic stem cells in vitro. Cold Spring Harb Protoc 2009: pdb prot5156. [PubMed: 20147086]
20. Kim D, Langmead B, and Salzberg SL. 2015 HISAT: a fast spliced aligner with low memory requirements. Nat Methods 12: 357–360. [PubMed: 25751142]
21. R-Core-Team. 2018 R: A language and environment for statistical computing. R Foundation for Statistical Computing, Vienna, Austria.
22. Love MI, Huber W, and Anders S. 2014 Moderated estimation of fold change and dispersion for RNA-seq data with DESeq2. Genome Biol 15: 550. [PubMed: 25516281]
23. Wickham H 2016 ggplot2: Elegant Graphics for Data Analysis. Springer-Verlag New York.
24. Risso D, Schwartz K, Sherlock G, and Dudoit S. 2011 GC-content normalization for RNA-Seq data. BMC Bioinformatics 12: 480. [PubMed: 22177264]
25. Zhu A, Ibrahim JG, and Love MI. 2018 Heavy-tailed prior distributions for sequence count data: removing the noise and preserving large differences. bioRxiv.
26. de Boer J, Williams A, Skavdis G, Harker N, Coles M, Tolaini M, Norton T, Williams K, Roderick K, Potocnik AJ, and Kioussis D. 2003 Transgenic mice with hematopoietic and lymphoid specific expression of Cre. Eur J Immunol 33: 314–325. [PubMed: 12548562]
27. Hodson DJ, Janas ML, Galloway A, Bell SE, Andrews S, Li CM, Pannell R, Siebel CW, MacDonald HR, De Keersmaecker K, Ferrando AA, Grutz G, and Turner M. 2010 Deletion of the RNA-binding proteins ZFP36L1 and ZFP36L2 leads to perturbed thymic development and T lymphoblastic leukemia. Nat Immunol 11: 717–724. [PubMed: 20622884]
28. Rongvaux A, Galli M, Denanglaire S, Van Gool F, Dreze PL, Szpirer C, Bureau F, Andris F, and Leo O. 2008 Nicotinamide phosphoribosyl transferase/pre-B cell colony-enhancing factor/visfatin is required for lymphocyte development and cellular resistance to genotoxic stress. J Immunol 181: 4685–4695. [PubMed: 18802071]
29. Coffey F, Lee SY, Buus TB, Lauritsen JP, Wong GW, Joachims ML, Thompson LF, Zuniga-Pflucker JC, Kappes DJ, and Wiest DL. 2014 The TCR ligand-inducible expression of CD73 marks gammadelta lineage commitment and a metastable intermediate in effector specification. J Exp Med 211: 329–343. [PubMed: 24493796]
30. Prinz I, Sansoni A, Kissenpfennig A, Ardouin L, Malissen M, and Malissen B. 2006 Visualization of the earliest steps of gammadelta T cell development in the adult thymus. Nat Immunol 7: 995–1003. [PubMed: 16878135]
31. Haas JD, Gonzalez FH, Schmitz S, Chennupati V, Fohse L, Kremmer E, Forster R, and Prinz I. 2009 CCR6 and NK1.1 distinguish between IL-17A and IFN-gamma-producing gammadelta effector T cells. Eur J Immunol 39: 3488–3497. [PubMed: 19830744]
32. Ribot JC, deBarros A, Pang DJ, Neves JF, Peperzak V, Roberts SJ, Girardi M, Borst J, Hayday AC, Pennington DJ, and Silva-Santos B. 2009 CD27 is a thymic determinant of the balance between interferon-gamma- and interleukin 17-producing gammadelta T cell subsets. Nat Immunol 10: 427–436. [PubMed: 19270712]
33. Holm M, Thomsen M, Hoyer M, and Hokland P. 1998 Optimization of a flow cytometric method for the simultaneous measurement of cell surface antigen, DNA content, and in vitro BrdUrd incorporation into normal and malignant hematopoietic cells. Cytometry 32: 28–36. [PubMed: 9581621]
34. Collins N, Poot RA, Kukimoto I, Garcia-Jimenez C, Dellaire G, and Varga-Weisz PD. 2002 An ACF1-ISWI chromatin-remodeling complex is required for DNA replication through heterochromatin. Nat Genet 32: 627–632. [PubMed: 12434153]
35. Mombaerts P, Clarke AR, Rudnicki MA, Iacomini J, Itohara S, Lafaille JJ, Wang LL, Ichikawa Y, Jaenisch R, Hooper ML, and Tonegawa S. 1992 Mutations in T-Cell Antigen Receptor Genes

Alpha-Block and Beta-Block Thymocyte Development at Different Stages. Nature 360: 225–231. [PubMed: 1359428]

36. Shinkai Y, and Alt FW. 1994 CD3 epsilon-mediated signals rescue the development of CD4+CD8+ thymocytes in RAG-2−/− mice in the absence of TCR beta chain expression. Int Immunol 6: 995–1001. [PubMed: 7947468]
37. Azzam HS, Grinberg A, Lui K, Shen H, Shores EW, and Love PE. 1998 CD5 expression is developmentally regulated by T cell receptor (TCR) signals and TCR avidity. J Exp Med 188: 2301–2311. [PubMed: 9858516]
38. Rodewald HR, Awad K, Moingeon P, D'Adamio L, Rabinowitz D, Shinkai Y, Alt FW, and Reinherz EL. 1993 Fc gamma RII/III and CD2 expression mark distinct subpopulations of immature CD4-CD8- murine thymocytes: in vivo developmental kinetics and T cell receptor beta chain rearrangement status. J Exp Med 177: 1079–1092. [PubMed: 8096236]
39. Teague TK, Tan C, Marino JH, Davis BK, Taylor AA, Huey RW, and Van De Wiele CJ. 2010 CD28 expression redefines thymocyte development during the pre-T to DP transition. Int Immunol 22: 387–397. [PubMed: 20203098]
40. Barnden MJ, Allison J, Heath WR, and Carbone FR. 1998 Defective TCR expression in transgenic mice constructed using cDNA-based alpha- and beta-chain genes under the control of heterologous regulatory elements. Immunol Cell Biol 76: 34–40. [PubMed: 9553774]
41. Kim J, Lee SK, Jeon Y, Kim Y, Lee C, Jeon SH, Shim J, Kim IH, Hong S, Kim N, Lee H, and Seong RH. 2014 TopBP1 deficiency impairs V(D)J recombination during lymphocyte development. EMBO J 33: 217–228. [PubMed: 24442639]
42. Alvarez JD, Yasui DH, Niida H, Joh T, Loh DY, and Kohwi-Shigematsu T. 2000 The MAR-binding protein SATB1 orchestrates temporal and spatial expression of multiple genes during T-cell development. Genes Dev 14: 521–535. [PubMed: 10716941]
43. He S, Limi S, McGreal RS, Xie Q, Brennan LA, Kantorow WL, Kokavec J, Majumdar R, Hou H Jr., Edelmann W, Liu W, Ashery-Padan R, Zavadil J, Kantorow M, Skoultchi AI, Stopka T, and Cvekl A. 2016 Chromatin remodeling enzyme Snf2h regulates embryonic lens differentiation and denucleation. Development 143: 1937–1947. [PubMed: 27246713]
44. Subramanian A, Tamayo P, Mootha VK, Mukherjee S, Ebert BL, Gillette MA, Paulovich A, Pomeroy SL, Golub TR, Lander ES, and Mesirov JP. 2005 Gene set enrichment analysis: a knowledge-based approach for interpreting genome-wide expression profiles. Proc Natl Acad Sci U S A 102: 15545–15550. [PubMed: 16199517]
45. Mingueneau M, Kreslavsky T, Gray D, Heng T, Cruse R, Ericson J, Bendall S, Spitzer MH, Nolan GP, Kobayashi K, von Boehmer H, Mathis D, Benoist C, Immunological Genome C, Best AJ, Knell J, Goldrath A, Joic V, Koller D, Shay T, Regev A, Cohen N, Brennan P, Brenner M, Kim F, Nageswara Rao T, Wagers A, Heng T, Ericson J, Rothamel K, Ortiz-Lopez A, Mathis D, Benoist C, Bezman NA, Sun JC, Min-Oo G, Kim CC, Lanier LL, Miller J, Brown B, Merad M, Gautier EL, Jakubzick C, Randolph GJ, Monach P, Blair DA, Dustin ML, Shinton SA, Hardy RR, Laidlaw D, Collins J, Gazit R, Rossi DJ, Malhotra N, Sylvia K, Kang J, Kreslavsky T, Fletcher A, Elpek K, Bellemare-Pelletier A, Malhotra D, and Turley S. 2013 The transcriptional landscape of alphabeta T cell differentiation. Nat Immunol 14: 619–632. [PubMed: 23644507]
46. Godfrey DI, Stankovic S, and Baxter AG. 2010 Raising the NKT cell family. Nat Immunol 11: 197–206. [PubMed: 20139988]
47. Rolink A, Grawunder U, Winkler TH, Karasuyama H, and Melchers F. 1994 IL-2 receptor alpha chain (CD25, TAC) expression defines a crucial stage in pre-B cell development. Int Immunol 6: 1257–1264. [PubMed: 7526894]
48. Jacks T, Remington L, Williams BO, Schmitt EM, Halachmi S, Bronson RT, and Weinberg RA. 1994 Tumor spectrum analysis in p53-mutant mice. Curr Biol 4: 1–7. [PubMed: 7922305]
49. Gebuhr TC, Kovalev GI, Bultman S, Godfrey V, Su L, and Magnuson T. 2003 The role of Brg1, a catalytic subunit of mammalian chromatin-remodeling complexes, in T cell development. J Exp Med 198: 1937–1949. [PubMed: 14676303]
50. Lan L, Ui A, Nakajima S, Hatakeyama K, Hoshi M, Watanabe R, Janicki SM, Ogiwara H, Kohno T, Kanno S, and Yasui A. 2010 The ACF1 complex is required for DNA double-strand break repair in human cells. Mol Cell 40: 976–987. [PubMed: 21172662]

51. Toiber D, Erdel F, Bouazoune K, Silberman DM, Zhong L, Mulligan P, Sebastian C, Cosentino C, Martinez-Pastor B, Giacosa S, D'Urso A, Naar AM, Kingston R, Rippe K, and Mostoslavsky R. 2013 SIRT6 recruits SNF2H to DNA break sites, preventing genomic instability through chromatin remodeling. Mol Cell 51: 454–468. [PubMed: 23911928]
52. Nakamura K, Kato A, Kobayashi J, Yanagihara H, Sakamoto S, Oliveira DV, Shimada M, Tauchi H, Suzuki H, Tashiro S, Zou L, and Komatsu K. 2011 Regulation of homologous recombination by RNF20-dependent H2B ubiquitination. Mol Cell 41: 515–528. [PubMed: 21362548]
53. Smeenk G, Wiegant WW, Marteijn JA, Luijsterburg MS, Sroczynski N, Costelloe T, Romeijn RJ, Pastink A, Mailand N, Vermeulen W, and van Attikum H. 2013 Poly(ADP-ribosyl)ation links the chromatin remodeler SMARCA5/SNF2H to RNF168-dependent DNA damage signaling. J Cell Sci 126: 889–903. [PubMed: 23264744]
54. Helmink BA, and Sleckman BP. 2012 The response to and repair of RAG-mediated DNA double-strand breaks. Annu Rev Immunol 30: 175–202. [PubMed: 22224778]
55. Bartek J, Lukas C, and Lukas J. 2004 Checking on DNA damage in S phase. Nat Rev Mol Cell Biol 5: 792–804. [PubMed: 15459660]
56. Baus F, Gire V, Fisher D, Piette J, and Dulic V. 2003 Permanent cell cycle exit in G2 phase after DNA damage in normal human fibroblasts. EMBO J 22: 3992–4002. [PubMed: 12881433]
57. Bunz F, Dutriaux A, Lengauer C, Waldman T, Zhou S, Brown JP, Sedivy JM, Kinzler KW, and Vogelstein B. 1998 Requirement for p53 and p21 to sustain G2 arrest after DNA damage. Science 282: 1497–1501. [PubMed: 9822382]
58. Krenning L, Feringa FM, Shaltiel IA, van den Berg J, and Medema RH. 2014 Transient activation of p53 in G2 phase is sufficient to induce senescence. Mol Cell 55: 59–72. [PubMed: 24910099]
59. Wurster AL, and Pazin MJ. 2012 ATP-dependent chromatin remodeling in T cells. Biochem Cell Biol 90: 1–13. [PubMed: 21999456]
60. Chi TH, Wan M, Lee PP, Akashi K, Metzger D, Chambon P, Wilson CB, and Crabtree GR. 2003 Sequential roles of Brg, the ATPase subunit of BAF chromatin remodeling complexes, in thymocyte development. Immunity 19: 169–182. [PubMed: 12932351]
61. Williams CJ, Naito T, Arco PG, Seavitt JR, Cashman SM, De Souza B, Qi X, Keables P, Von Andrian UH, and Georgopoulos K. 2004 The chromatin remodeler Mi-2beta is required for CD4 expression and T cell development. Immunity 20: 719–733. [PubMed: 15189737]
62. Morris SA, Baek S, Sung MH, John S, Wiench M, Johnson TA, Schiltz RL, and Hager GL. 2014 Overlapping chromatin-remodeling systems collaborate genome wide at dynamic chromatin transitions. Nat Struct Mol Biol 21: 73–81. [PubMed: 24317492]
63. Sala A, Toto M, Pinello L, Gabriele A, Di Benedetto V, Ingrassia AM, Lo Bosco G, Di Gesu V, Giancarlo R, and Corona DF. 2011 Genome-wide characterization of chromatin binding and nucleosome spacing activity of the nucleosome remodelling ATPase ISWI. EMBO J 30: 1766–1777. [PubMed: 21448136]

KEY POINTS:

A. ISWI ATPase Smarca5 guide developmental mRNA program of β-selected thymocytes

B. Inactivation of *Smarca5* gene in developing thymocytes activates p53 and apoptosis

C. Smarca5 regulates cell fate decisions of γδ thymocytes and survival of proB cells.

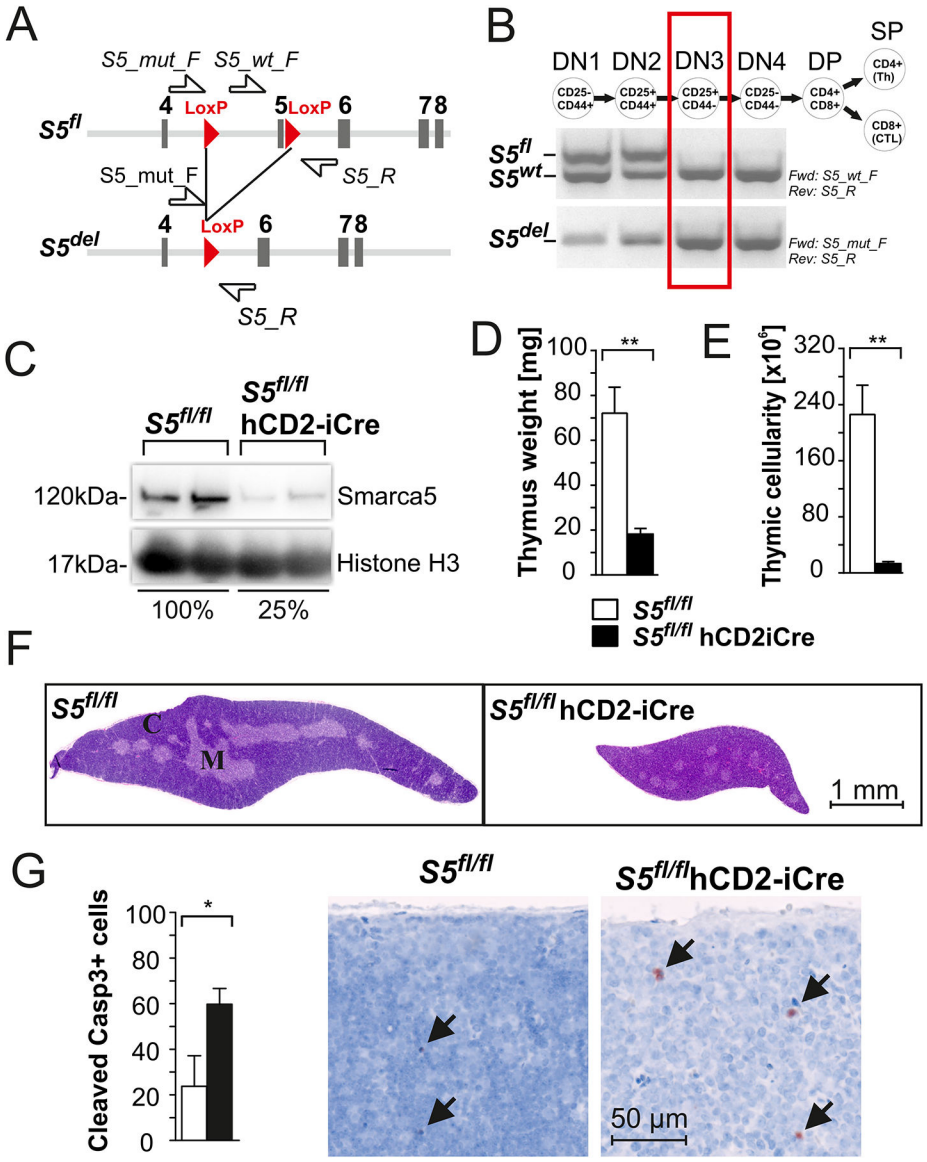

Figure 1. Smarca5 is required for thymocyte development and survival.

(**A**) Scheme of Cre-mediated deletion in the *Smarca5* gene. Indicated are exons 4–8 (boxes), positions of loxP1 sites (red triangles), and positions of genotyping primers (white arrows). (**B**) PCR detection of the floxed ($S5^{fl}$), wild-type ($S5^{wt}$) and deleted ($S5^{del}$) *Smarca5* allele in the DN cell subsets isolated from $S5^{fl/wt}$hCD2iCre thymus. (**C**) Immunoblot showing Smarca5 protein expression in thymi of control (one animal per sample) versus $S5^{fl/fl}$hCD2iCre (a pool of four animals per sample) mice. Histone H3 served as a loading control. (**D, E**) Weight and cellularity of thymi of indicated genotypes. Bars depict the mean ± SD from four controls and four $S5^{fl/fl}$hCD2iCre mice. (**F**) Histology (H&E staining) of thymi from 6-week-old mice of indicated genotypes showing medulla (M) and cortex (C). (**G**) Immunohistochemistry of cleaved Caspase-3 in Mayer's hematoxylin stained thymic sections. Y-axis: mean number/mm^2 ± SD of cleaved Casp3 positive cells in the cortex (n=3/genotype); Significance in two-tail t-test (*p<0.05, **p<0.01, ***p<0.001, ****p<0.0001).

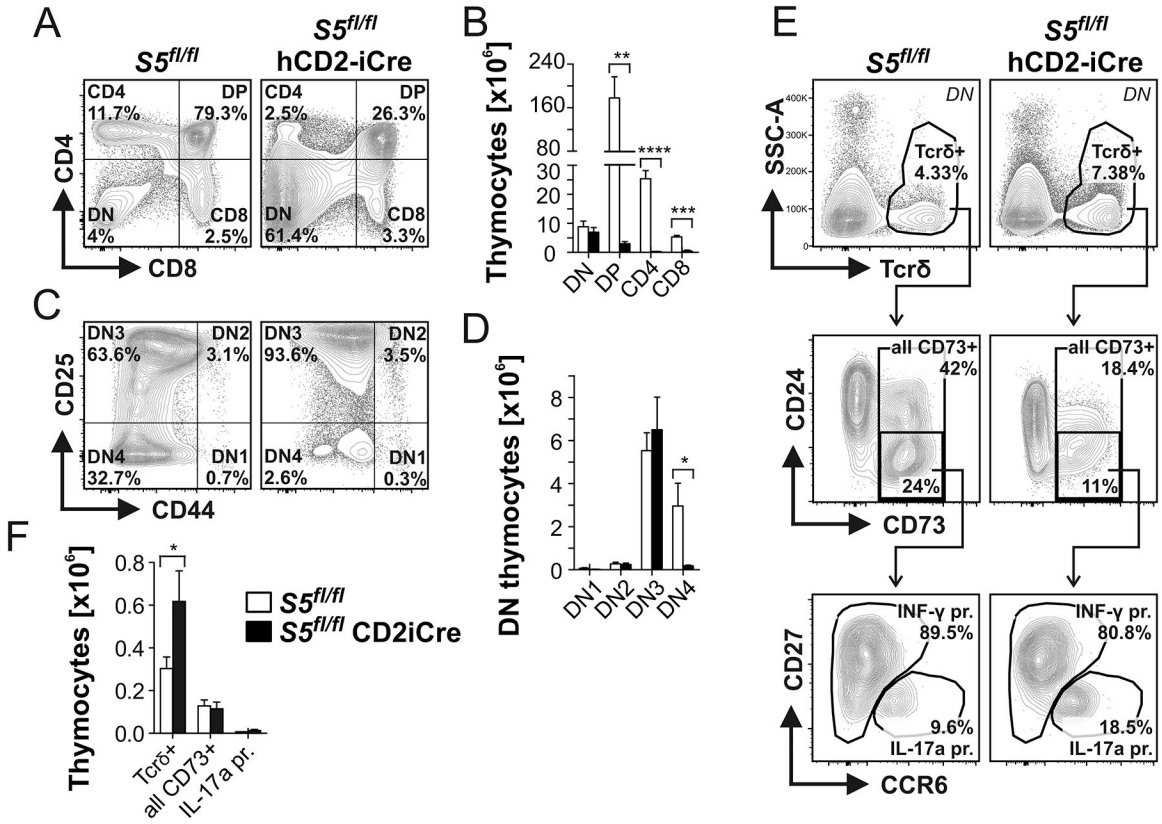

Figure 2. Smarca5 is required for thymocyte development at DN3 to DN4 stage.

(**A, B**) Flow cytometry analysis of CD4 and CD8 double negative (DN), double positive (DP) and single positive (SP) cell populations in thymi of 4–6 week-old control (n=4) and *S5*$^{fl/fl}$hCD2iCre (n=4) mice. Relative (**A**) and absolute (**B**) quantitation of thymic fraction sizes are shown. (**C, D**) Flow cytometry analysis of thymic DN (CD4^{-}CD8^{-}) cells of indicated genotypes using anti-CD25 and CD44 staining shown as relative (**C**) or absolute (**D**) values. Bars graphs depict the mean ± SD from 4 controls and 4 *S5*$^{fl/fl}$hCD2iCre mice (same animals as in A and B). Lineage-positive (B220, Gr-1, CD11b, CD11c, and Nk1.1) cells were excluded from all measurements. (**E, F**) Flow cytometry analysis of γδT cells in DN (CD4^{-}CD8^{-}) thymic fraction. (**E**) Expression profiles of surface markers are shown as a contour plots and the proportions of cells within each gate are given. (**F**) Bars graphs depict the mean ± SD of absolute numbers. Data are representative of 3 control and 3 *S5*$^{fl/fl}$hCD2iCre animals. Significance in two-tailed t-test; *p<0.05, **p<0.01, ***p<0.001, ****p<0.0001.

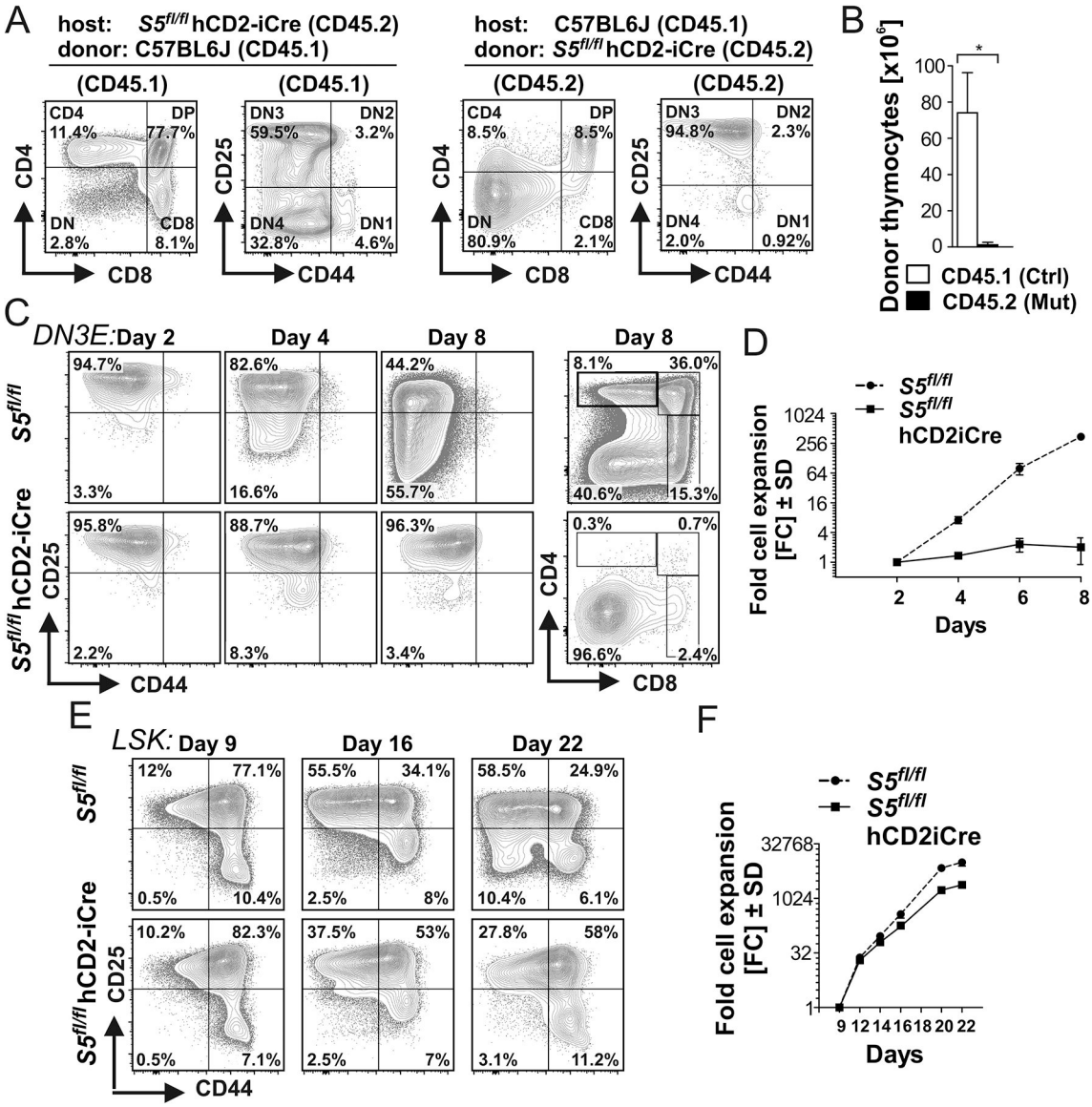

Figure 3. Developmental blockade in Smarca5-deficient thymocytes is cell-autonomous.

(**A**) Flow cytometric evaluation of donor-derived thymic populations regenerated after one month following the transplantation of donor bone marrow cells (BMT) into lethally irradiated (7.5Gy) hosts. Donor and host-derived thymocytes were distinguished by surface expression of distinct variants of marker CD45. Control mice were CD45.1$^+$ (Ly5.1) and *S5$^{fl/fl}$*hCD2iCre were CD45.2$^+$ (Ly5.2). Data are representative of three BMT experiments. (**B**) Bar diagram shows mean number ± SD of donor (CD45.1 = wild-type; CD45.2 = *S5$^{fl/fl}$*hCD2iCre) thymocytes one month after BMT. Data are representative of three experiments. (**C**) FACS sorted DN3e (small CD4$^-$CD8$^-$CD25$^+$) thymocytes from control and *S5$^{fl/fl}$*hCD2iCre mice were co-cultured with OP9/N-DLL1 stromal cell line. Cells were harvested on days 2, 4, 8 and expression profiles of CD44/CD25 or CD4/CD8 markers were analyzed by flow cytometry. Data are representative of two experiments. (**D**) Cumulative growth curve (represented as fold-change) of all live CD45$^+$ cells isolated from OP9/N-

DLL1 co-cultures on days 2, 4, 6, 8. Cells were the same as in C. (**E**) Flow cytometry of purified $Lin^{-}Sca1^{+}c\text{-}Kit^{+}$ (LSK) bone marrow progenitors after 9, 16 and 22 days of cultivation with OP9/N-DLL1 cells. Data are representative of 4 control and 4 $S5^{fl/fl}$hCD2iCre animals. (**F**) Cumulative growth curve (represented as fold-change) of cells analyzed in E.

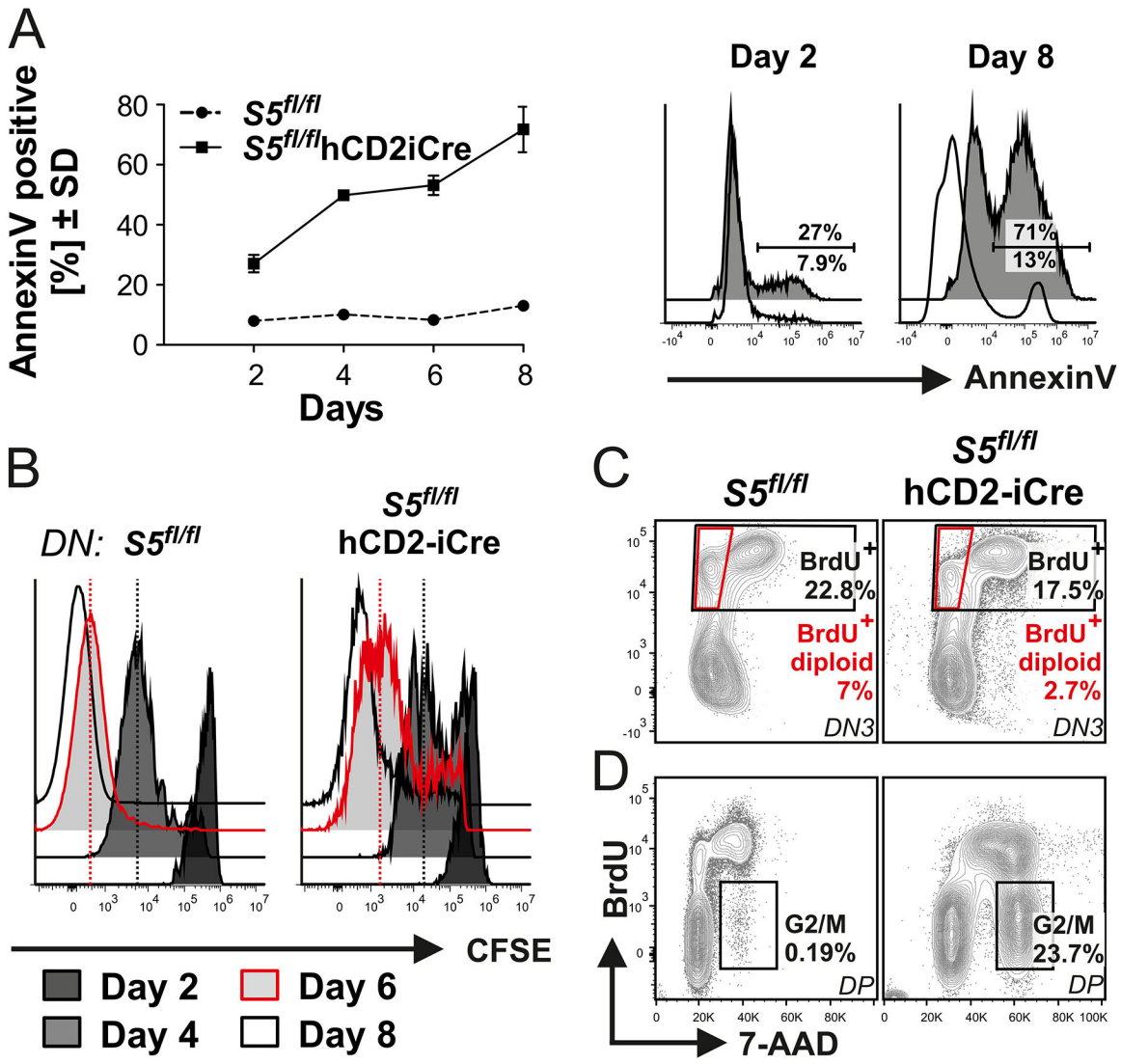

Figure 4. Smarca5-deficient thymocytes induce apoptosis and block proliferation.

(**A**) Purified preselection DN3e thymocytes (from 2 animals of each genotype) were cocultured with OP9/N-DLL1 cells and mean fraction ± SD of $CD45^+$ cells that became Annexin V positive was assessed by flow cytometry following 2, 4, 6 and 8 days. Histograms (blank = control mice; gray, filled histogram = $S5^{fl/fl}$hCD2iCre mice) show results of the experiments at day 2 and 8. (**B**) Histograms of control and $S5^{fl/fl}$hCD2iCre DN thymocytes stained with carboxyfluorescein succinimidyl ester (CFSE) fluorescent cell dye and cocultured with OP9/N-DLL1 cells. CFSE signal dilution was analyzed by flow cytometry on days 2, 4, 6 and 8. Data are representative of four control and three $S5^{fl/fl}$hCD2iCre animals. (**C**) Flow cytometry analysis of control and $S5^{fl/fl}$hCD2iCre DN3 population cell cycle progression using Bromodeoxyuridine (BrdU)/7-aminoactinomycin D (7AAD) double staining. Black rectangles depict all gated $BrdU^+$ cells. Red trapezoid indicates $BrdU^+$ diploid postreplicative cells that accomplished the mitosis. (**D**) Flow cytometry for BrdU and 7-AAD in DP cells. Rectangles show the proportion of G2/M fraction. Data are representative of at least 3 individual animals of each genotype.

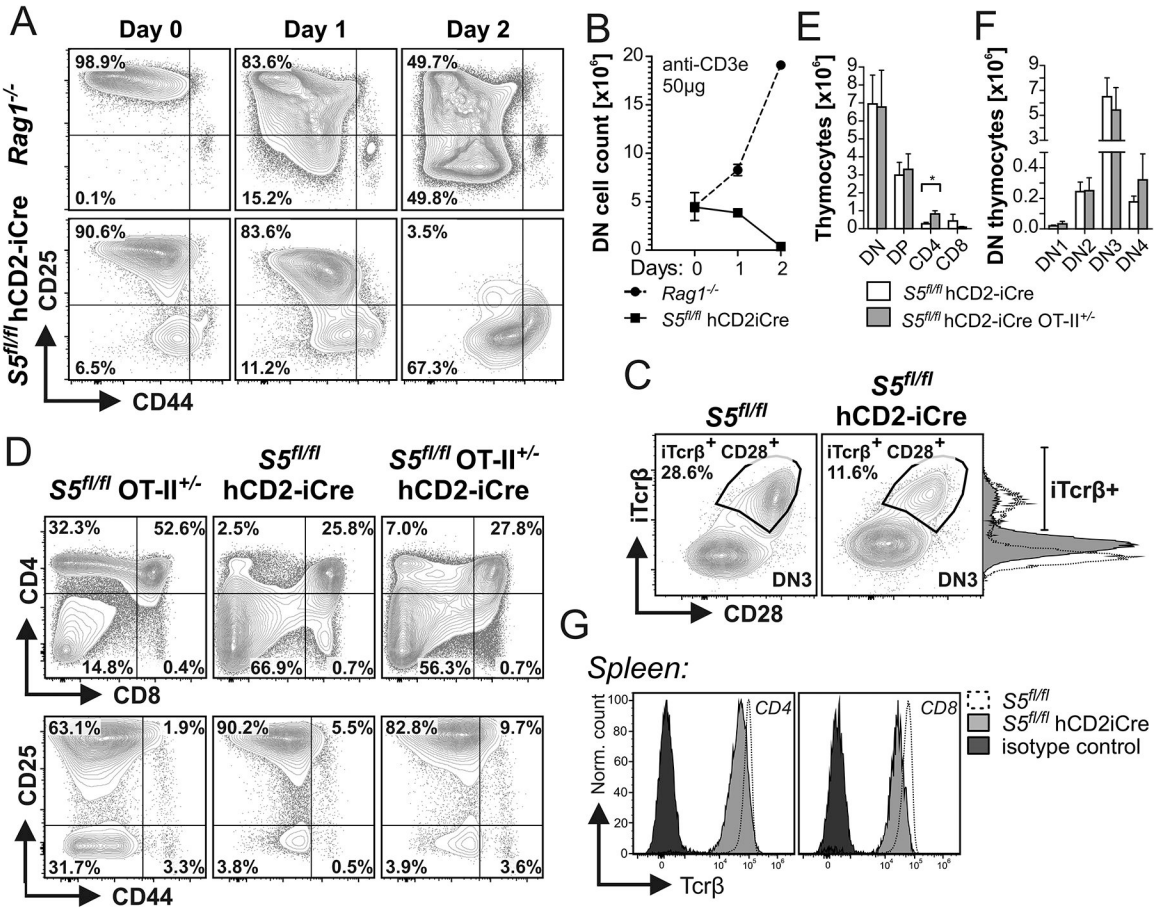

Figure 5. Smarca5 is not required for pre-TCR signaling and the TCR rearrangement.

(**A**) Flow cytometry analysis of differentiation markers on thymocytes isolated 1 day and 2 days after intraperitoneal injection of *Rag1*$^{-/-}$ and *S5*$^{fl/fl}$hCD2iCre mice with anti-CD3 (50µg/mice); Contour plots showing DN (CD4^{-}CD8^{-}) cells. Data are representative of five (day 0), two (day 1) and three (day 2) *Rag1*$^{-/-}$ or *S5*$^{fl/fl}$hCD2iCre animals. (**B**) Mean of absolute numbers ± SD of cells isolated from the thymus of mice used in A. (**C**) Contour plots showing expression of CD28 and intracellular Tcrβ (iTcrβ) in DN3 thymocytes of indicated genotypes. Data are representative of three experiments. (**D**) Flow cytometry of DN, DP and SP fractions using CD4 and CD8 markers in thymic suspensions from 4–6 week-old *S5*$^{fl/fl}$ OT-II$^{+/-}$ control, *S5*$^{fl/fl}$hCD2iCre and *S5*$^{fl/fl}$hCD2iCre OT-II$^{+/-}$ mice. The relative population sizes are indicated. DN thymocytes were analyzed for CD25 and CD44 marker expressions. All B220, Gr-1, Mac-1, CD11c and Nk1.1 lineage positive cells were excluded from the analysis. Data are representative of more than three experiments. (**E, F**) Mean of absolute numbers ± SD of thymic subpopulations as in D. Two-tail t-test; *p<0.05. (**G**) Surface expression of Tcrβ protein on CD4 and CD8 T cells of control and *S5*$^{fl/fl}$hCD2iCre animals analyzed by flow cytometry. As an isotype control to H57–597 clone (anti-Tcrβ) was used fluorescently labeled Armenian Hamster IgG (dark histograms). Data are representative of three experiments.

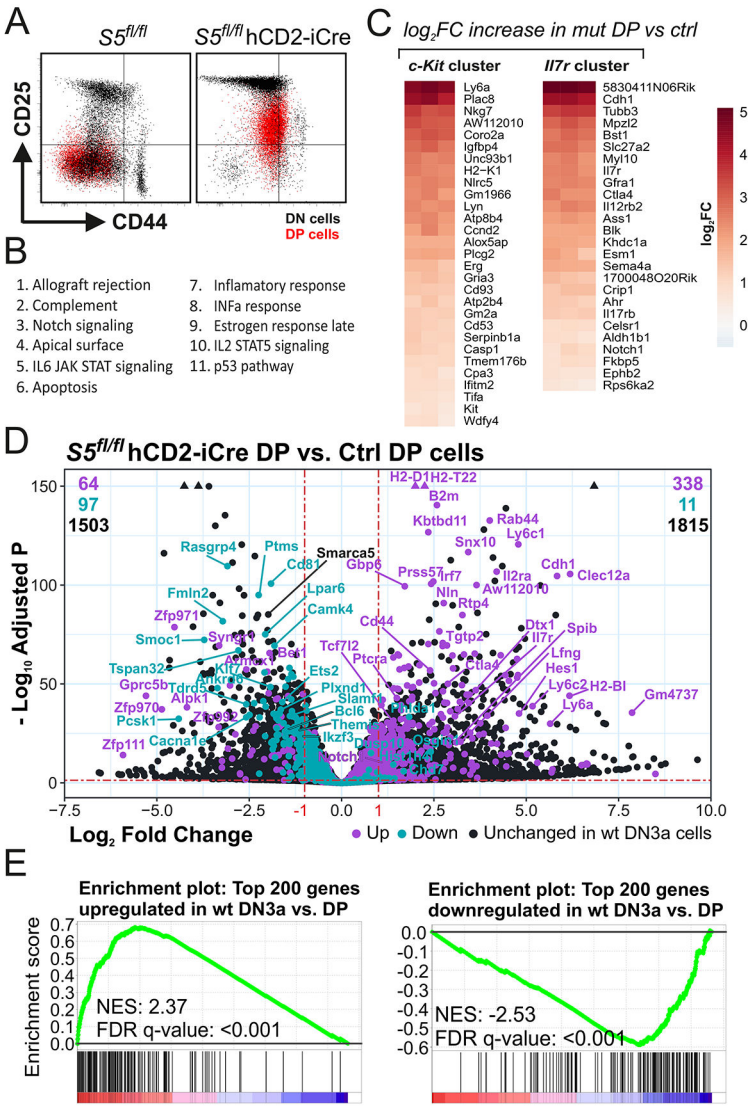

Figure 6. Smarca5 deficiency altered the developmental program of post-*β*-selection stages.

(**A**) Flow cytometry of thymus. Dot plot shows analysis of CD25 and CD44 marker expressions on the surface of CD4/CD8 double negative (DN, black dots) and overlapping double positive (DP, red dots) thymocytes. (**B**) The list of 11 most significantly enriched Hallmark gene sets in Molecular Signatures Database v6.2 by GSEA. (**C**) Heat maps of upregulated genes (log_2FC scale) in *S5*$^{fl/fl}$ hCD2iCre mutant DP cells vs. control *S5*$^{fl/fl}$ DP thymocytes. The *c-Kit* and *Il7r* gene clusters were defined previously using microarray analysis of thymocyte development (45). Gene expression profile heatmaps represent three individual experiments from sorted DP cells, each pooled from 25–37 *S5*$^{fl/fl}$ hCD2iCre animals and normalized to controls (n=3). (**D**) Data from RNA-seq presented as Volcano plot. The X-axis represents log_2 fold change in expression of mutant DP cells as compared to the control (*S5*$^{fl/fl}$) DP cells. The Y-axis represents *adjusted p-value* (p_{adj}). The horizontal dashed line is equal to p_{adj} = 0.05). Genes (as green dots) are those that are normally

downregulated in DN3a cells and become upregulated in DP cells during development and vice versa the violet gene dots are upregulated in DN3a and during development become downregulated (based on microarray analysis of thymocytes Mingueneau *et al.* 2013). Numbers in upper corners indicate numbers of differentially expressed genes between mutant and control of each gene set within $\log_2$FC of <−1 or >1. (**E**) Enrichment analysis of differentially expressed genes in $S5^{fl/fl}$hCD2iCre DP thymocytes vs. control DP cells (same as in D) was performed on the two gene sets containing 200 most upregulated (left plot) and downregulated (right plot) transcripts in wild-type DN3a compared to wild-type DP stage thymocytes (according to (45)). For the complete list of genes pertaining to each of the gene sets see Supplemental Figure 2A. Positive (left plot) GSEA enrichment score curve indicates that the genes comprising the leading edge of the GSEA plot (mostly DN3a abundant transcripts) are positively correlated with mutant $S5^{fl/fl}$hCD2iCre DP cells. Similarly, for downregulated genes, the GSEA indicated a correlation between $S5^{fl/fl}$hCD2iCre DP cells and normal DN3a cells (lower plot). NES, Normalized enrichment score.

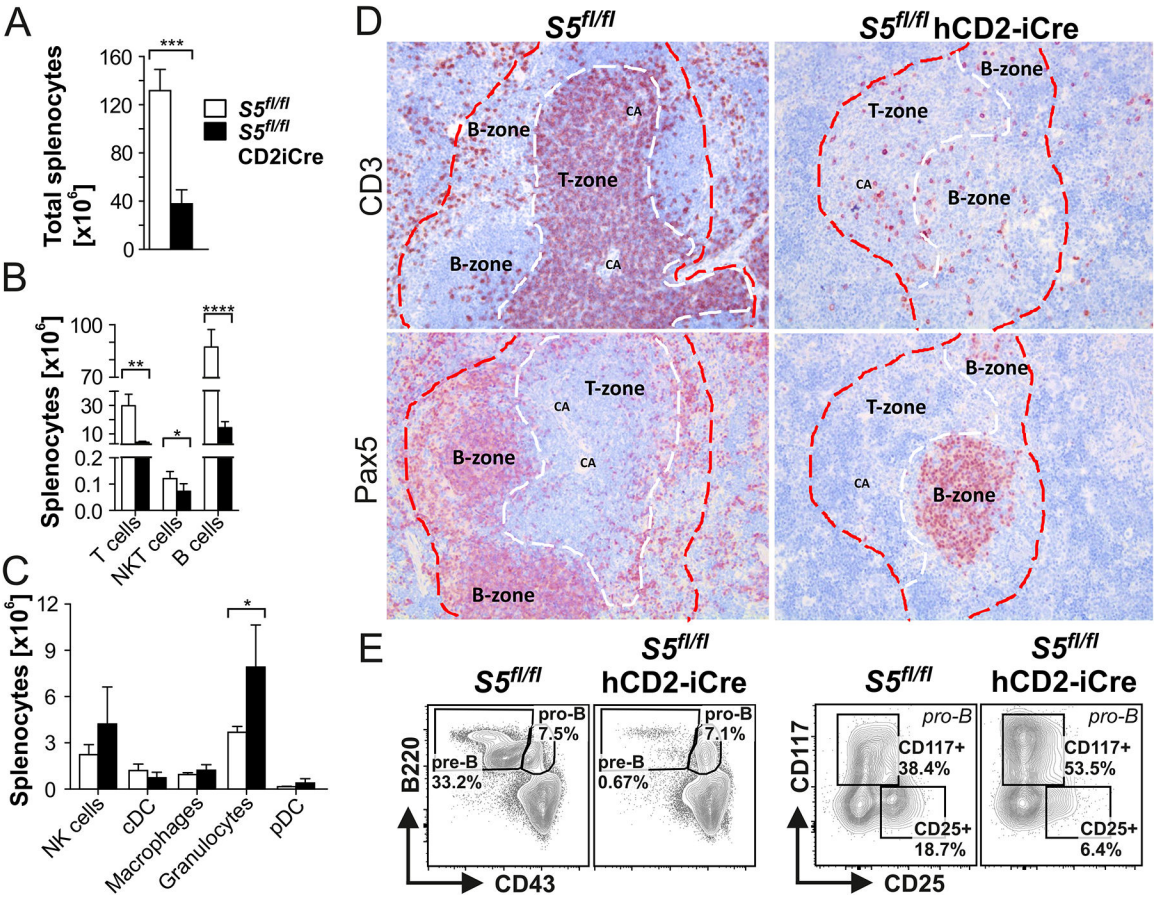

Figure 7. Smarca5-deficient B cell progenitors are arrested at proB/preB transition.

(**A**) Bar diagrams show the mean number ± SD of CD45$^+$ cells or (**B**) peripheral lymphocytes or (**C**) myeloid cells in spleens of control (n=5) and *S5*$^{fl/fl}$hCD2iCre (n=5) mice. Two-tail t-test; *p<0.05, **p<0.01, ***p<0.001, ****p<0.0001. (**D**) Immunohistochemistry for CD3 (T cell marker) and Pax5 (B cell marker) in the spleen of 6-week old control or *S5*$^{fl/fl}$hCD2iCre mice. Data are representative of three experiments. CA - central arterioles (**E**) Flow cytometry analysis of early B cell subpopulation in BM of control or *S5*$^{fl/fl}$hCD2iCre mice. Left plots show B220 and CD43 staining of all Ter119 negative cells in BM. Right plots show CD117 and CD25 staining of CD43$^+$B220$^+$ (pro-B) cells gated in upper plots. Data are representative of six control and nine *S5*$^{fl/fl}$hCD2iCre animals.

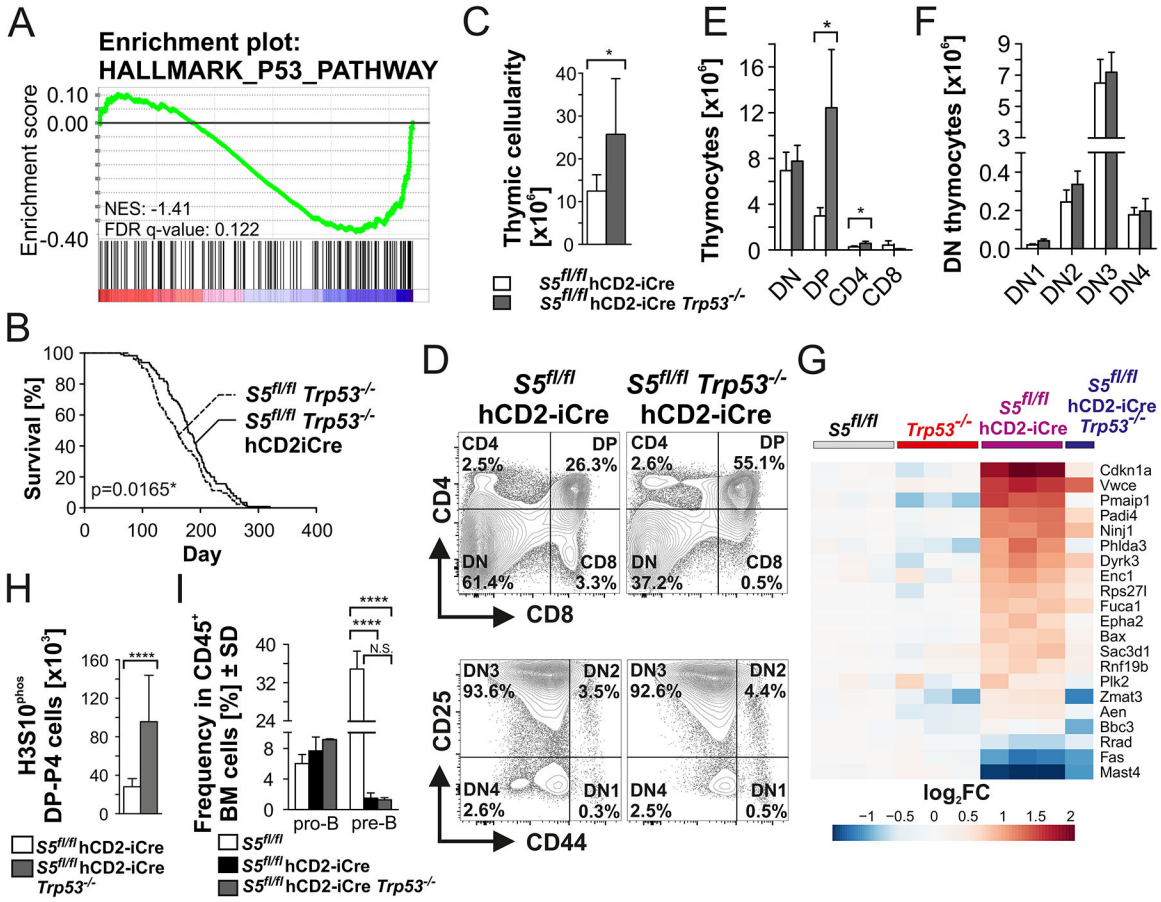

Figure 8. *Trp53* co-deletion rescues survival but not differentiation of Smarca5-deficient thymocytes.

(**A**) GSEA showing a representative enrichment plot of genes involved in p53 pathways and networks comparing DP thymocytes sorted from *S5*$^{fl/fl}$hCD2iCre (three individual pools, see Fig. 6C) mice vs. DP thymocytes isolated from *S5*$^{fl/fl}$ controls (n=3). Negative GSEA enrichment score curve indicates that the genes comprising the leading edge of the GSEA plot are positively correlated with mutant *S5*$^{fl/fl}$hCD2iCre DP cells. (**B**) Kaplan-Meier survival curve of controls (dashed line, n=125) and *Smarca5/Trp53* double mutants (n=115). Log-rank (Mantel-Cox) test used; *p<0.05. (**C**) Bars depict the mean of absolute numbers ± SD of thymocytes from *S5*$^{fl/fl}$hCD2iCre (n=4) and *S5*$^{fl/fl}$hCD2iCre *Trp53*$^{-/-}$ (n=5) mice. (**D**) Flow cytometric plots showing distributions of thymic CD4/CD8 positive and negative developmental stages of indicated genotypes. The CD4/CD8 double negative cells were further distinguished using CD25 and CD44 surface markers (lower graphs). Lineage-positive (B220, Gr-1, Mac-1, Nk1.1, CD11c, Ter119) cells were excluded from all measurements. Data are representative of four *S5*$^{fl/fl}$hCD2iCre and five *S5*$^{fl/fl}$hCD2iCre *Trp53*$^{-/-}$ animals. (**E, F**) Mean of absolute numbers ± SD of thymic subpopulations as in D. Two-tail t-test; *p<0.05. (**G**) Heat map showing expression of genes which were differentially regulated in *S5*$^{fl/fl}$hCD2iCre mice but normally expressed in *S5*$^{fl/fl}$hCD2iCre *Trp53*$^{-/-}$ animals compare to controls and *Trp53*$^{-/-}$ mice. The expression is normalized to controls; $\log_2$ scale. The last column represents gene expression profiles of pooled DP cells sorted from 6 *S5*$^{fl/fl}$hCD2iCre *Trp53*$^{-/-}$ animals. (**H**) Absolute counts of mitotic phospho-

histone H3 (Ser10) positive DP cells in *S5*$^{fl/fl}$hCD2iCre and *S5*$^{fl/fl}$hCD2iCre *Trp53*$^{-/-}$ double knock-outs. Two-tail t-test; ****p<0.0001. (**I**) Relative numbers of early B cell subpopulations in BM of indicated genotypes. Data are normalized to all CD45^{+} cells and represent mean of at least three animals. Two-tail t-test; *p<0.05, ****p<0.0001.